

# Selenium Nanoparticles-Enriched *Lactobacillus casei* ATCC 393 Prevents Cognitive Dysfunction in Mice Through Modulating Microbiota-Gut-Brain Axis

Lei Qiao, Yue Chen, Xiaofan Song, Xina Dou, Chunlan Xu 

The Key Laboratory for Space Bioscience and Biotechnology, School of Life Sciences, Northwestern Polytechnical University, Xi'an, People's Republic of China

Correspondence: Chunlan Xu, The Key Laboratory for Space Bioscience and Biotechnology, School of Life Sciences, Northwestern Polytechnical University, Xi'an, People's Republic of China, Tel +86 29-88460543, Fax +86 29-88460332, Email clxu@nwpu.edu.cn

**Purpose:** The bidirectional communication between the gut and the central nervous system mediated by gut microbiota is closely related to the occurrence and development of neurodegenerative diseases, including Alzheimer's disease (AD). Selenium (Se) has been identified as playing a role against AD. Probiotics have beneficial effects on host brain function and behavior by modulating the microbiota-gut-brain axis. Herein, we evaluated the protective effects of *Lactobacillus casei* ATCC 393 (*L. casei* ATCC 393) and selenium nanoparticles-enriched *L. casei* ATCC 393 (*L. casei* ATCC 393-SeNPs) against D-galactose/aluminum chloride-induced AD model mice.

**Methods:** The Morris Water Maze (MWM) test was used to assess cognitive function of mice. The morphology and histopathological changes, antioxidant capacity and immune responses in the brain and ileum were evaluated. The alterations in intestinal permeability of the mice were determined using FITC-dextran. Gut microbiota composition was assessed using 16s rRNA sequencing.

**Results:** Thirteen weeks intervention with *L. casei* ATCC 393 or *L. casei* ATCC 393-SeNPs significantly improved cognitive dysfunction, and minimized amyloid beta ( $A\beta$ ) aggregation, hyperphosphorylation of TAU protein, and prevented neuronal death by modulating Akt/cAMP-response element binding protein (CREB)/brain-derived neurotrophic factor (BDNF) signaling pathway. Moreover, compared with *L. casei* ATCC 393, *L. casei* ATCC 393-SeNPs further effectively mitigated intestinal barrier dysfunction by improving antioxidant capacity, regulating immune response, restoring gut microbiota balance, and increasing the level of short-chain fatty acids and neurotransmitters, thereby inhibiting the activation of microglia and protecting brain neurons from neurotoxicity such as oxidative stress and neuroinflammation.

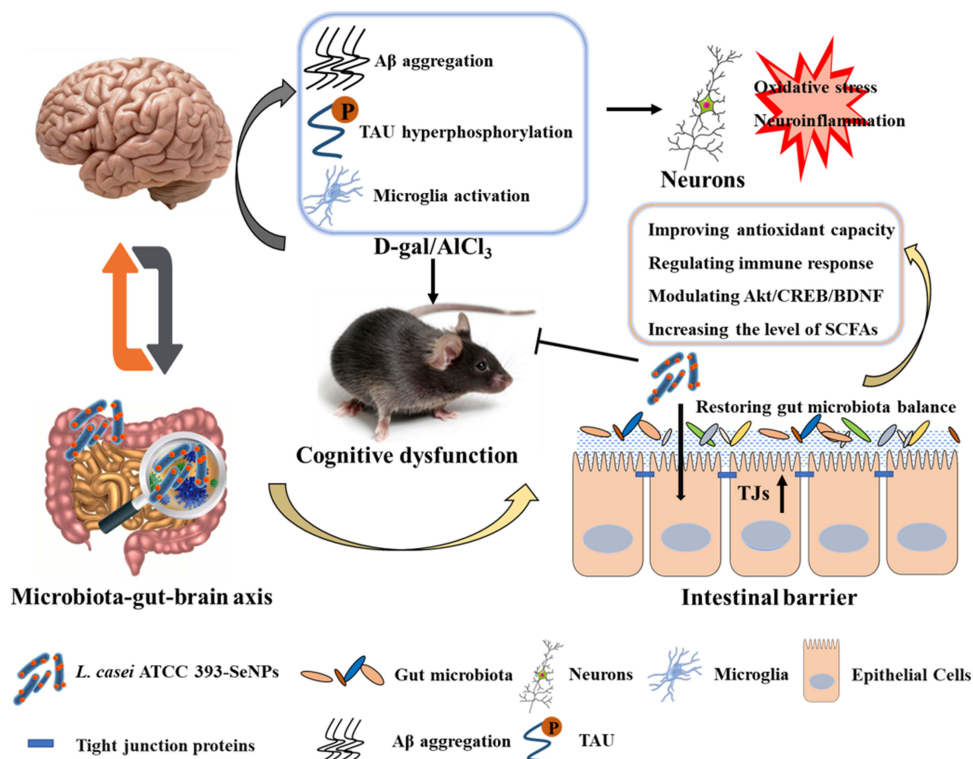
**Conclusion:** These findings indicated that targeting the microbiota-gut-brain axis with *L. casei* ATCC 393-SeNPs may have therapeutic potential for the deficits of cognitive function in the AD model mice. Thus, we anticipate that *L. casei* ATCC 393-SeNPs may be a promising and safe Se nutritional supplement for use as a food additive to prevent the neurodegenerative disease.

**Keywords:** neurodegenerative disease, gut microbiota, oxidative stress, neuroinflammation

## Introduction

Alzheimer's disease (AD) is a chronic neurodegenerative disease with complex pathogenesis, and its main clinical manifestations are cognitive and memory impairment and progressive impairment of activities of daily living.<sup>1</sup> As a multifactorial disease caused by a combination of own factors, genetic conditions and environmental influences, AD has so far neither an effective cure nor any treatment. The development of amyloid beta ( $A\beta$ ) plaques, neurofibrillary tangles, oxidative stress, neuroinflammation, and mitochondrial dysfunction are the hallmarks of AD.<sup>2</sup> The representative pathological markers in AD patients are the accumulation of insoluble  $A\beta$  and hyperphosphorylated TAU in the brain, where the excessive deposition of  $A\beta$  plays a significant role in the pathogenesis of AD.<sup>3</sup> Recently, the level of  $A\beta$  was reported to be positively correlated with the levels of oxidation products of proteins, lipids, and nucleic acids in the hippocampus and cortex.<sup>4</sup> In addition, mitochondria dysfunction has also been involved in AD pathogenesis through

## Graphical Abstract



mitochondrial ROS generation.<sup>5</sup> Meanwhile, the deposition of Aβ drives brain neuroinflammation by activating microglia, which further stimulates the production of pro-inflammatory cytokines in the brains of AD patients.<sup>6</sup> Therefore, inhibition of Aβ plaque-associated pathophysiology, including oxidative stress and neuroinflammation is a promising strategic direction to delay AD progression.

Accumulating evidence suggested that AD pathological features and cognitive-behavioral abilities are associated with gut microbiota dysbiosis.<sup>7</sup> The gut microbiota of AD patients exhibits lower microbial diversity and is significantly different in composition from healthy individuals, and this change results in differences in the metabolites of gut microbiota.<sup>8</sup> Vogt et al performed a comprehensive sequencing analysis of fecal samples from AD patients and found that the microbiome of AD patients had a reduced microbial richness and diversity, with a unique composition compared with normal individuals. At the phylum level, the abundance of *Firmicutes* and *Actinobacteria* significantly decreased, while *Bacteroidetes* were enriched in AD patients. At the genus level, *Bifidobacterium*, *Clostridium*, etc. were less abundant, while the abundance of *Blautia*, *Phascolarctobacterium*, *Gemella*, *Bacteroides*, *Alistipes*, and *Bilophila* were all high in AD patients. Furthermore, the abundance of these bacteria correlates closely with biomarkers of AD pathology, suggesting that altered AD microbiome can be linked to neuropathological changes in AD.<sup>9</sup> Another study found lower abundance of *Eubacterium rectale* and higher abundance of *Shigella* in amyloid-positive patients.<sup>10</sup> In addition, gut microbiota imbalance can lead to the secretion of large amounts of amyloids, lipopolysaccharides and inflammatory-related molecules, and damage the intestinal mucosal barrier, contributing to the activation of microglia and triggering neuroinflammation in the central nervous system, potentially contributing to the neurodegeneration.<sup>11</sup> Increased intestinal permeability promotes the translocation and accumulation of metabolites that promote microglial dysfunction.<sup>12</sup> Toll-like receptor 4 (TLR4) is an important pattern recognition receptor associated with inflammation, and in brain tissue, TLR4 is mainly expressed in microglia. Activation of TLR4 and its downstream pathways can promote

the activation of microglia and the release of inflammatory factors in the brain.<sup>13</sup> The gut microbiota metabolite lipopolysaccharide (LPS) is an important activator of TLR4, which can specifically bind to TLR4 and activate its downstream pro-inflammatory signaling pathway.<sup>14</sup> Huo et al found that increases in intestinal permeability and plasma LPS levels were positively correlated with the expression of inflammatory cytokines in the brain of mice. In addition, gut barrier protectors (intestinal alkaline phosphatase) that reduce plasma LPS levels can effectively ameliorate neuroinflammation in mice. Therefore, increased LPS translocation caused by intestinal barrier dysfunction may be an important cause of microglia activation.<sup>15</sup> Thus, the concept of the microbiota-gut-brain axis was proposed based on the bidirectional communication between the gut microbiota and the brain, which is achieved through the immune system, the vagus nerve, the enteric nervous system, and microbial metabolites, including short-chain fatty acids (SCFAs), proteins, and tryptophan metabolites.<sup>16</sup> Recently, studies have found that probiotics administration improved central nervous system-related diseases, such as AD, autism and depressive disorder.<sup>17–19</sup> Akbari et al found that a probiotic combination containing *Lactobacillus acidophilus*, *Lactobacillus casei*, *Bifidobacterium bifidum*, and *Lactobacillus fermentum* positively affects cognitive function and metabolic status in AD patients.<sup>20</sup> In an exploratory intervention study using probiotic supplementation in AD patients, multispecies probiotics treatment altered gut microbiota composition and serum tryptophan metabolism. After treatment, compared with control group, treatment with probiotic patients had lower intestinal permeability and increased the abundance of *Faecalibacterium prausnitzii*, a SCFAs-producing microorganism.<sup>21</sup> A meta-analysis suggested that probiotics may improve cognitive performance in AD or mild cognitive impairment (MCI) patients by decreasing levels of neuroinflammation and oxidative stress.<sup>22</sup> These results indicated the potential efficacy of probiotics in improving cognitive dysfunction in AD patients.<sup>23</sup>

Micronutrient selenium (Se) plays a key role in redox regulation through its incorporation into selenoproteins. Studies have shown a direct relationship between Se deficiency in serum and hair samples and memory impairment in AD patients.<sup>24</sup> Tamtaji et al found that multiple probiotics and Se combination improved mini-mental state examination (MMSE) score and metabolic profiles in AD patients.<sup>25</sup> In addition, sodium selenate supplementation at high or supranutritional doses increases Se uptake into the central nervous system and that subtle but significant improvement in MMSE scores.<sup>26</sup> However, sodium selenite has the characteristics of high toxicity, low biological activity, narrow range of safe supplementation, and is not easy to be absorbed and utilized by the human body, etc., and is not suitable for wide application in medicine and food.<sup>27</sup> Recently, Se nanoparticles (SeNPs) have received extensive attention due to their low toxicity, high bioavailability, and high bioactivity.<sup>28</sup> In addition, the results of safety evaluation based on cell and animal models have indicated that the toxicity of Se species is ranked as follows: selenate>selenite>selenomethionine>SeNPs.<sup>27</sup> Our previous study demonstrated that SeNPs synthesized by *Lactobacillus casei* ATCC 393 (*L. casei* ATCC 393) possess significant antioxidant and anti-inflammatory activities in vitro and in vivo and dietary supplementation with SeNPs can prevent oxidative stress-induced intestinal barrier dysfunction through its regulation of gut microbiota.<sup>29–31</sup> Moreover, our latest research found that biogenic SeNPs synthesized by *L. casei* ATCC 393 can effectively alleviate the A $\beta$ <sub>25–35</sub>-induced apoptosis of PC12 cells. Therefore, this study was conducted to investigate the preventive effects of SeNPs-enriched *L. casei* ATCC 393 (*L. casei* ATCC 393-SeNPs) on the AD mice model induced by D-galactose (D-gal)/aluminum chloride (AlCl<sub>3</sub>) and its relationship with microbiota-gut-brain axis.

## Materials and Methods

### Reagents

*L. casei* ATCC 393-SeNPs were prepared according to our previously established methods. Specifically, *L. casei* ATCC 393 was incubated with 1.2 mM sodium selenite for 24 h under anaerobic conditions to obtain biomolecules capped-SeNPs with particle sizes of 50 and 80 nm.<sup>29</sup> The experimental diets were obtained from Trophic Animal Feed High-tech Co., Ltd. (Suzhou, China). The Se-deficient diet (0.0-Se) contained Se at a level <0.015 mg/kg. The *L. casei* ATCC 393 diet was enriched with *L. casei* ATCC 393 (0.5×10<sup>9</sup> CFU/g). The *L. casei* ATCC 393-SeNPs diet was enriched with *L. casei* ATCC 393-SeNPs, the final Se content was 0.3 mg/kg, and the *L. casei* ATCC 393 content was 0.5×10<sup>9</sup> CFU/g. FITC-dextran (4 kDa) and AlCl<sub>3</sub> were obtained from Sigma-Aldrich (Saint Louis, MO, USA). D-gal, thioredoxin reductase (TrxR) activity assay kit (cat# BC1155), glutathione peroxidase (GPx) activity assay kit (cat# BC1195),

superoxide dismutase (SOD) assay kit (cat# BC0175), malondialdehyde (MDA) assay kit (cat# BC0025) and acetylcholinesterase (AChE) assay kit (cat# BC2025) were purchased from Beijing Solarbio Science & Technology Co., Ltd. (Beijing, China). ELISA kits for interleukin-1 $\beta$  (IL-1 $\beta$ , cat# JL18442), interleukin-4 (IL-4, cat# JL20266), interleukin-10 (IL-10, cat# JL20242), interleukin-18 (IL-18, cat# JL20253), amyloid beta 1–42 (A $\beta$ <sub>1–42</sub>, cat# JL11386), 5-hydroxytryptamine (5-HT, cat# JL12087), dopamine (DA, cat# JL11187) and  $\gamma$ -aminobutyric acid (GABA, cat# JL12094) were purchased from Jianglaibio Company (Shanghai, China). Primary antibodies for  $\beta$ -actin (cat# AC026), bax (cat# A0207), bcl-2 (cat# A0208), p53 (cat# A5761), caspase1 (cat# A0964) and brain-derived neurotrophic factor (BDNF, cat# A1307) and secondary antibody for HPR goat anti-rabbit IgG (cat# AS014) were purchased from ABclonal Biotechnology (Wuhan, China). Primary antibodies for Akt (cat# BS1007), pAkt (cat# BS4006), cAMP-response element binding protein (CREB, cat# BS6230) and pCREB (cat# BS4781) were purchased from Bioworld Technology, Inc. (Bloomington, USA). The ionized calcium-binding adapter molecule 1 (IBA-1, cat# GB11105) antibody used for immunohistochemical assay was purchased from Servicebio (Wuhan, China).

## Animal Experimental Design

The animal experiment was approved by the Institutional Animal Care and Use Committee of the Northwestern Polytechnical University (Xi'an, China, No. 202,101,085) and conducted in accordance with the National Institutes of Health guidelines for the care and use of experimental animals. A total of 40 male C57BL/6 mice aged 8 weeks (body weight: 21.65  $\pm$  0.72 g) were purchased from the Beijing Vital River Laboratory Animal Technology Co., Ltd. (Beijing, China). After a week of adaptation, all mice were randomly assigned to four groups with 10 mice per group: the control group (Se-deficient diet), the AD model group (Se-deficient diet), the L393 group (*L. casei* ATCC 393 diet) and the L393-SeNPs group (*L. casei* ATCC 393-SeNPs diet). The mice in each group ate the above diets *ad libitum* throughout the experimental period (13 weeks). From the fifth week, the mice in AD model, L393 and L393-SeNPs groups were modeled by intraperitoneal injection of D-gal (150 mg/kg body weight) and oral gavage of AlCl<sub>3</sub> (20 mg/kg body weight) once daily for 8 weeks. Also, animals received equal amounts of normal saline as a healthy control. And on the last 1 week, the mice were subjected to behavioral studies.

## Morris Water Maze

The Morris Water Maze (MWM) test was used to assess cognitive function of mice. MWM consists of a circular water pool (150 cm in diameter, 50 cm in height) and an escape platform (10 cm in diameter) 1 cm below the water surface, located in the center of the fourth quadrant of the pool. The water was changed to white by adding white pigment, and the water temperature was kept around 23  $\pm$  1°C. Each mouse was placed in four different start quadrants to find the hidden platform (up to 120 s) and allowed to stay on there for 20s for five consecutive training days (four trails per day). The test was conducted on the sixth day, and the platform was removed. Each mouse was allowed to start from the opposite quadrant of the target and searched for the site of the original platform (freely explore for 120 s, and record the trajectories within 120 s). Escape latency time, movement speed, time near platform, number of passes through platform, and the representative track of the test were recorded by the automated software (Beijing Zhongshi Dichuang Technology Development Co., Ltd.).

## H&E and Nissl Staining

The morphology and histopathological changes in the brain and ileum were evaluated by hematoxylin and eosin (H&E) staining and Nissl staining. The brain and ileum were fixed in 4% paraformaldehyde and embedded in paraffin. Subsequent tissue sections were stained with H.E. or toluidine blue staining according to standard procedures.<sup>31</sup> Images of the slices were obtained using inverted microscope (Leica DMIL, Germany).

## Immunohistochemical Assay

Paraffin-embedded brain sections were deparaffinized in xylene, and rehydrated in graded ethanol. Then, the tissue sections are placed in a repair box filled with citric acid (pH 6.0) antigen retrieval buffer for antigen retrieval. Subsequently, sections were placed in 3% hydrogen peroxide and incubated at room temperature for 25 min in the

dark to block endogenous peroxidase activity. After blocking with 3% bovine serum albumin for 30 min, the slices were incubated with a primary antibody against IBA-1 (1:300) at 4 °C overnight, after which they were incubated with the Signal Stain Boost immunohistochemical detection reagent (HRP, Rabbit) at room temperature for 30 min. Finally, the sections were stained with the 3,3'-diaminobenzidine (DAB) liquid substrate system. Images of the slices were obtained using inverted microscope (Leica DMIL, Germany).

## Quantitative Analysis of Neurotransmitters and A $\beta$ <sub>1-42</sub>

The levels of 5-HT, DA, GABA, and A $\beta$ <sub>1-42</sub> in serum or brain were measured by corresponding mouse ELISA kit according to the manufacturer's instructions.

## AchE Activity Detection

The activity of AchE was determined using the AchE activity assay kit according to the manufacturer's instructions.

## Intestinal Permeability Test

The alterations in intestinal permeability of the mice were determined using FITC-dextran (4 kDa). 4 h prior to the end of the experiment, mice were given 400 mg/kg B.W. of FITC-dextran by gavage,<sup>31</sup> and the concentration of FITC-dextran in serum was measured with a Multi-Mode Microplate Reader (Bio-Rad, Hercules, USA).

## Se Content Detection

The Se content in the organs, serum and feces were measured by inductively coupled plasma-mass spectrometry (ICP-MS). About 200 mg of samples were dissolved with 5 mL of mixed acid (HNO<sub>3</sub>: HClO<sub>4</sub> = 4:1) until the solution was colorless and transparent. The solution was then heated at 100°C for 2 h to volatilize the acid. Finally, the sample solutions were transferred to a 10 mL volumetric flask for ICP-MS.

## Antioxidant Capacity and Immune Responses Detection

The level of MDA, and the T-SOD, GPx and TrxR activities in serum, brain and ileum were determined using the corresponding kits according to the manufacturer's instructions. The levels of IL-1 $\beta$ , IL-18, IL-4 and IL-10 in the serum, brain and ileum were measured by the corresponding ELISA kits according to the manufacturer's instructions.

## Gut Microbiota and Metabolism Analysis

Total genomic DNA samples were extracted using the OMEGA Soil DNA Kit (M5635-02) (Omega Bio-Tek, Norcross, GA, USA), following the manufacturer's instructions, and the quantity and quality of extracted DNAs were measured using a NanoDrop NC2000 spectrophotometer (Thermo Fisher Scientific, Waltham, MA, USA). After extracting the microbial community DNA, variable regions V3–V4 of bacterial 16S rRNA gene were amplified with degenerate PCR primers, 338F (5'-ACTCCTACGGGAGGCAGCA-3') and 806R (5'-GGACTACHVGGGTWTCTAAT-3'). Gut microbiota composition was assessed using Illumina MiSeq platform and QIIME2-based microbiota analysis in Shanghai Personal Biotechnology Co., Ltd (Shanghai, China).

The cecal contents were resuspended in a saturated NaCl solution. The samples were acidified with sulfuric acid (10%) and fatty acids were extracted with diethyl ether. The mixture was centrifuged at 12,000 rpm for 10 min and Na<sub>2</sub>SO<sub>4</sub> was then added to the supernatant to remove the water content. The concentrations of SCFAs in the samples were analyzed by gas chromatography-mass spectrometry (GC-MS) on a TRACE1300-TSQ9000 Triple Quadrupole GC-MS/MS System (Thermo Fisher Scientific, Waltham, MA, USA).

## Western Blot Analysis

Total protein was isolated from jejunum using the RIPA buffer (cat# P0013B; Beyotime, Shanghai, China) containing protease and phosphatase inhibitor cocktail (cat# C0001 and cat# C0002; Topscience, Shanghai China) and homogenized on ice. Next, the supernatants were collected after centrifugation at 13,000 g for 15 min at 4°C. The protein concentration of the samples was measured by the BCA protein assay kit (cat# DQ111-01; TransGen, Beijing, China).

Before loading, protein samples were boiled in the loading buffer, then samples of equal volume (20  $\mu$ L) with an equal amount (30  $\mu$ g) of protein and Multicolor Prestained Protein Ladder (cat# WJ103; Epizyme, Shanghai, China) were loaded onto the sodium dodecyl sulphate-polyacrylamide gel electrophoresis (SDS-PAGE) gel, and then transferred to the polyvinylidene difluoride (PVDF) membrane. The membranes were incubated overnight at 4°C with the appropriate primary antibodies for  $\beta$ -actin, TAU, pTAU, p53, Bcl-2, Bax, Caspase1, ZO-1, occludin, claudin1, Akt, pAkt, CREB, pCREB and BDNF followed by incubation for 1 h at room temperature with the appropriate secondary antibodies. Immunoreactive protein bands were visualized with the Clarity™ Western ECL Substrate kit (Bio-Rad, CA, USA) using chemiluminescence detection system (T5200Multi; Tanon, Shanghai, China) and exposed using TanonImage (Tanon, Shanghai, China). In the exposure process, we first use the automatic exposure function to expose. Then select an appropriate exposure time for exposure, usually only 1–5 seconds for the housekeeping protein and 1–3 minutes for the target proteins. Finally, quantitative analysis was performed using Image J analyzer software (National Institute of Health, Bethesda, USA).

## Statistical Analysis

The data are expressed as the mean  $\pm$  S.E.M. Statistical analysis was performed using the GraphPad Prism 7.0 software (GraphPad Software Inc., San Diego, CA, USA). One-way analysis of variance (ANOVA) followed by a least significant difference multiple comparison test was used to determine the statistical significance for multiple comparisons, and Student's *t*-test was used for the comparisons of two groups.  $P < 0.05$  was considered as statistically significant.

## Results

### Protective Effects of *L. casei* ATCC 393-SeNPs on Cognitive Dysfunction in AD Model Mice

As shown in the scheme (Figure 1A), co-administration of D-gal and  $AlCl_3$  were used to induce the AD-like mouse model. We compared the difference in body weight between groups of mice at the thirteenth week, compared with the control group, the average body weight of the mice in the AD model group decreased ( $p = 0.1631$ ), and the body weight of the AD model group was also lower than that in the *L. casei* ATCC 393 ( $p = 0.2247$ ) and *L. casei* ATCC 393-SeNPs ( $p = 0.3894$ ) groups. Moreover, the body weight of the mice in the *L. casei* ATCC 393-SeNPs group was slightly higher than that in the *L. casei* ATCC 393 group ( $p = 0.4838$ ), but the body weights were similar between the control and *L. casei* ATCC 393-SeNPs groups ( $p = 0.3755$ , Figure 1B). MWM test was used to assess cognitive function of mice. In the acquisition training, a gradual decline was noted in the escape latency among all groups. However, compared to the control group, AD model group exhibited significant memory deficits, manifested by prolonged escape latency, an increased swimming distance and slower movement speed to find the targeted quadrant in the 5 days navigation test. In addition, AD model mice treated with *L. casei* ATCC 393 and *L. casei* ATCC 393-SeNPs showed enhanced performance in shortening the escape latency, decreasing escape the swimming distance and accelerating movement speed, indicating the beneficial effect of *L. casei* ATCC 393 and *L. casei* ATCC 393-SeNPs in the process of learning and memory consolidation (Figure 1C–E). The probe trial was performed to assess the long-term memory of the animals six days after the training session. As shown in Figure 1F, after removing the underwater escape platform, the movement trajectories of the mice in each group were significantly different within 120 s. Except for the AD model group, the main movement range of the mice in the other three groups revolved around the quadrant (fourth quadrant) where the virtual platform (the original underwater platform was placed). In addition, compared with the control group, the AD model group significantly reduced the number of crossing the virtual platform during the experiment. Compared with AD model group, *L. casei* ATCC 393 and *L. casei* ATCC 393-SeNPs treatment significantly increased the number of passes through the platform and residence time on the virtual platform, reflecting improved spatial memory in AD model mice (Figure 1G and H). These findings demonstrated that *L. casei* ATCC 393-SeNPs attenuated AD-induced cognitive impairment.

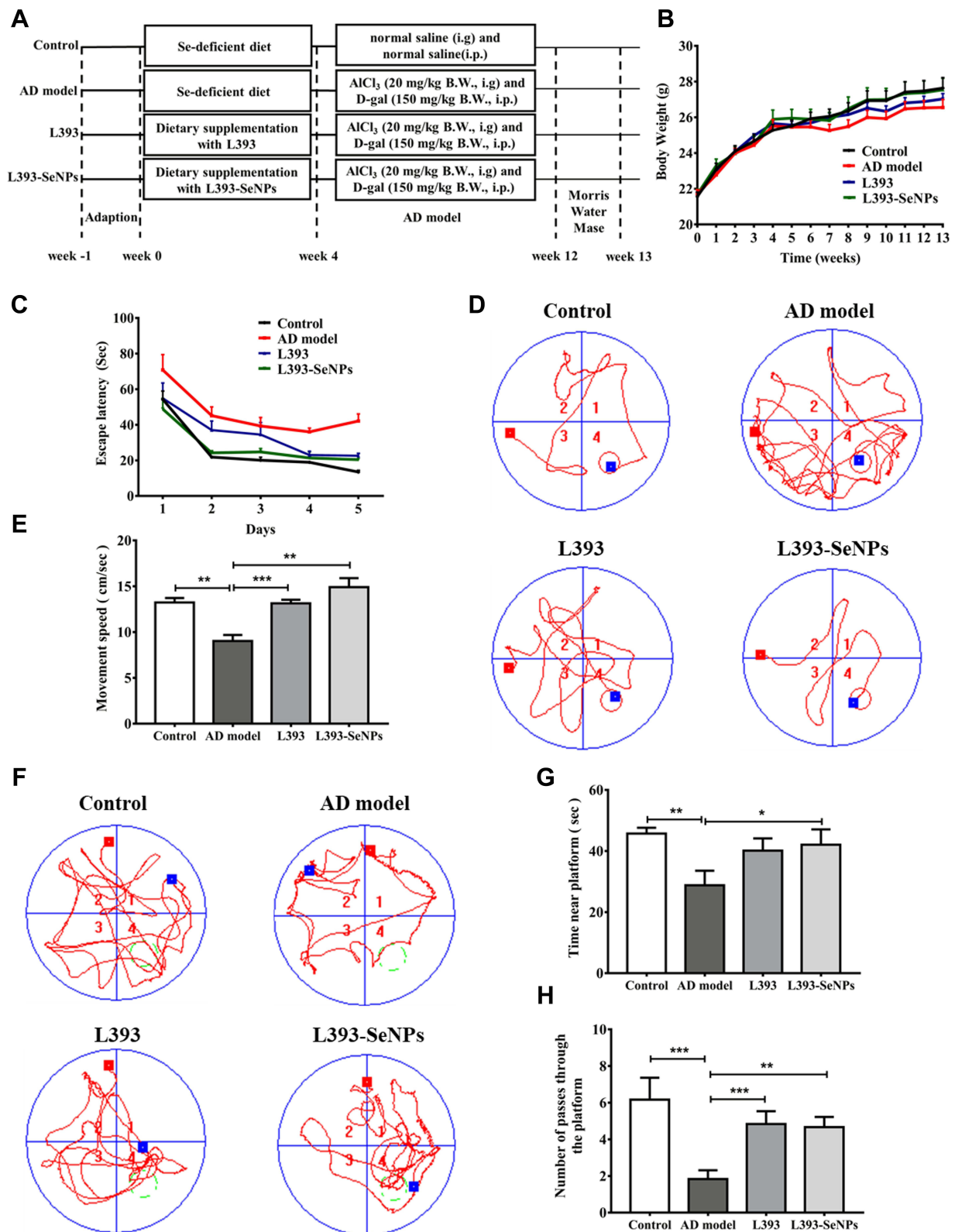


**Figure 1** Protective effects of *L. casei* ATCC 393-*SeNPs* on cognitive dysfunction in AD model mice. **(A)** Schematic diagram of experiment. **(B)** The average body weight of mice in each experimental group during the whole experiment period (n=10). **(C–H)** The cognitive functions and spatial memory of mice were evaluated by the MWM test. The escape latency **(C)** the representative track of the test **(D)** and movement speed **(E)** to the hidden platform during five training days. The representative track of the test **(F)**, the time near the target platform **(G)** and the number of passes through the platform **(H)** on day 6 (n=6). Data are represented as the mean  $\pm$  S.E.M. \* $P < 0.05$ ; \*\* $P < 0.01$ ; \*\*\* $P < 0.001$  (L393: *L. casei* ATCC 393; L393-*SeNPs*: *L. casei* ATCC 393-*SeNPs*).

## Effects of *L. casei* ATCC 393-SeNPs on Histopathological Changes and Neurotransmitters in the Serum and Brain of AD Model Mice

The histopathological changes in the hippocampus were observed by H&E staining of hippocampal CA1 region and Nissl staining of hippocampal dentate gyrus. As shown in **Figure 2A**, compared with control group, neuronal cells in AD model group showed the phenomenon of eosinophilic staining (black arrow), and accompanied by pyknotic nuclei. In addition, the arrangement of neurons was more disordered. Conversely, AD model mice treated with *L. casei* ATCC 393 and *L. casei* ATCC 393-SeNPs can significantly reduce the phenomenon of eosinophilic staining and maintain the normal morphology of neurons. The results of Nissl staining (red arrow) manifested that unlike the normal neuronal morphology in the control, abnormal morphologies were observed in the AD model mice, including a large number of damaged, illegible neurons that were loosely and irregularly arranged, and vacuolar-like structures appeared. However, dietary supplementation with *L. casei* ATCC 393 or *L. casei* ATCC 393-SeNPs groups effectively alleviated the hippocampal histopathological damage-induced by D-gal/ $\text{AlCl}_3$ . Furthermore, Nissl staining revealed that *L. casei* ATCC 393-SeNPs reduced impairment of neuronal integrity and fewer morphological changes compared to *L. casei* ATCC (Figure 2B). AD pathology is also related to abnormal neurotransmitter function, we further detected the levels of DA, GABA and 5-HT in the serum, brain and ileum of mice. Compared with the control group, the levels of DA and GABA in serum levels of GABA and 5-HT in brain, and the levels of

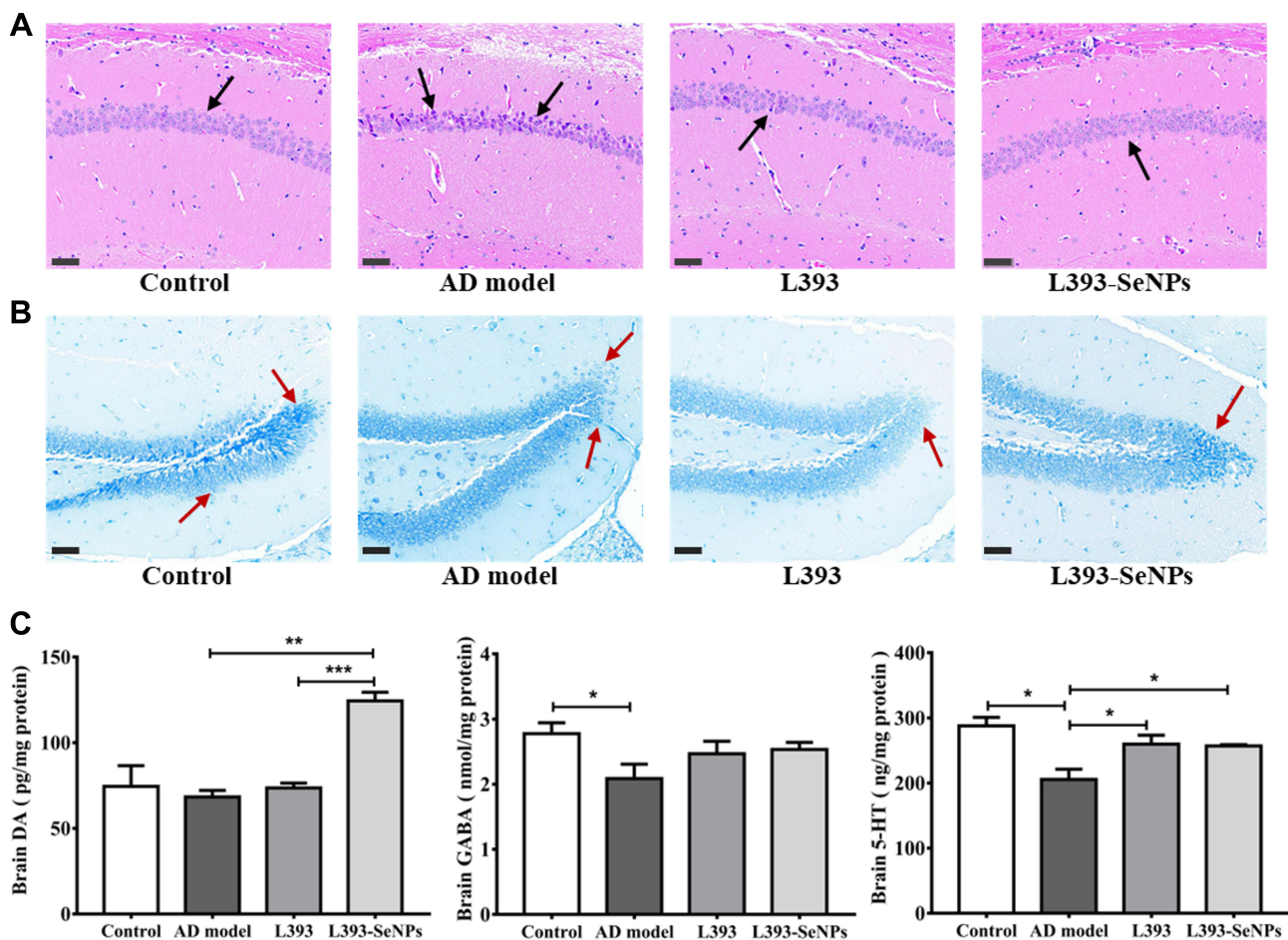


**Figure 2** Effects of *L. casei* ATCC 393-SeNPs treatment on histopathological changes and neurotransmitters in the serum and brain of AD model mice. **(A)** H&E staining of hippocampal CA1 region (Scale bar: 50  $\mu\text{m}$ ). Black arrows represent neurons in hippocampal CA1 area. Compared with the control group, the neurons in the CA1 region of the AD model group were disordered, the cytoplasm was dense, and the eosinophilic staining was enhanced, and the addition of *L. casei* ATCC 393-SeNPs to the diet could alleviate this phenomenon. **(B)** Nissl staining in the dentate gyrus of the hippocampus (Scale bar: 50  $\mu\text{m}$ ). Dentate gyrus neuronal cells are dark blue (red arrow). The neurons in the dentate gyrus of the mice in the control group had normal morphology, and the cells were arranged neatly and regularly; the cells in the AD model group were loosely arranged, some neurons were missing, and a large number of vacuolar-like structures appeared; compared with the model group, the L393-SeNPs group had complete cell morphology, arranged more neatly. **(C)** The levels of neurotransmitters (DA, GABA and 5-HT) in brain. Data are represented as the mean  $\pm$  S.E.M.  $n=6$ . \* $P < 0.05$ ; \*\* $P < 0.01$ ; \*\*\* $P < 0.001$  (L393: *L. casei* ATCC 393; L393-SeNPs: *L. casei* ATCC 393-SeNPs).

GABA and 5-HT in ileum of AD model group were significantly decreased. However, dietary *L. casei* ATCC 393 supplementation significantly increased the levels of GABA in serum, the level of 5-HT in brain and the levels of GABA and 5-HT in ileum of AD model group. Dietary *L. casei* ATCC 393-SeNPs supplementation can significantly increase the levels of DA and 5-HT in serum and brain, and the levels of DA, GABA and 5-HT in ileum of AD model group (Figure 2C, Figure S1A and B). These results demonstrated that *L. casei* ATCC 393 and *L. casei* ATCC 393-SeNPs facilitate the synthesis of neurotransmitters and protect the hippocampus from damage in AD model mice.

## Dietary Supplementation with *L. casei* ATCC 393-SeNPs Suppressed A $\beta$ Aggregation, TAU Hyperphosphorylation and Neuronal Apoptosis in AD Model Mice

Deposition of A $\beta$  protein is considered to be a major causative factor in the AD. The result showed that exogenous administration of D-gal and AlCl<sub>3</sub> significantly increased the content of A $\beta$ <sub>1-42</sub> in the mice brain. AD model mice treated with *L. casei* ATCC 393 and *L. casei* ATCC 393-SeNPs significantly reduced A $\beta$ <sub>1-42</sub> levels in the brain, and *L. casei* ATCC 393-SeNPs showed a stronger effect than *L. casei* ATCC 393 in reducing A $\beta$ <sub>1-42</sub> content. Even though *L. casei* ATCC 393-SeNPs reduced A $\beta$ <sub>1-42</sub> level in the brain, its levels did not decrease to control group (Figure 3A). AchE is an important functional enzyme of the cholinergic nervous system and can hydrolyze the neurotransmitter acetylcholine (Ach), thereby maintaining

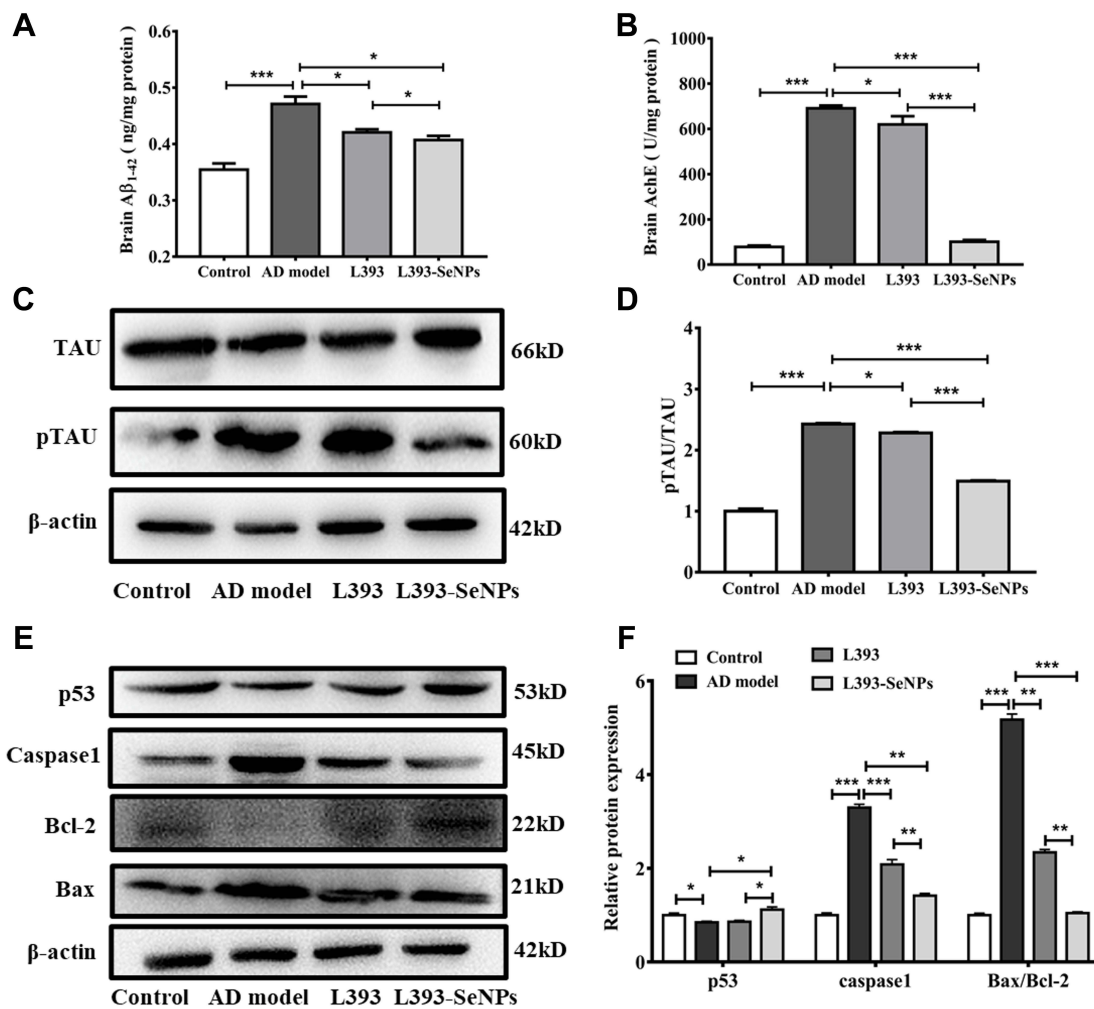


**Figure 3** Dietary *L. casei* ATCC 393-SeNPs supplementation suppressed A $\beta$  aggregation, TAU hyperphosphorylation and neuronal apoptosis in AD model mice. (A) The level of A $\beta$ <sub>1-42</sub> in brain. (B) The activity of AchE in brain. (C) The expression levels of TAU and pTAU detected by Western blot analysis. (D) Quantitative analysis of the protein expression level of pTAU/TAU. (E) The expression levels of apoptosis-related proteins (p53, caspase-1, Bax and Bcl-2) detected by Western blot analysis. (F) Quantitative analysis of the protein expression levels of p53, caspase-1 and Bax/Bcl-2. Data are represented as the mean  $\pm$  S.E.M. n=4. \*P < 0.05; \*\*P < 0.01; \*\*\*P < 0.001 (L393: *L. casei* ATCC 393; L393-SeNPs: *L. casei* ATCC 393-SeNPs).

the stability of nervous system function.<sup>32</sup> Therefore, detecting the activity of AchE can indirectly determine the content of Ach in the brain. As shown in Figure 3B, compared with the control group, the AchE activity in the brain of the AD model mice was significantly increased. However, the AchE activity in L393 and L393-SeNPs groups was decreased compared with the AD model group, and the effect of *L. casei* ATCC 393-SeNPs was more pronounced, which reduced the AchE activity to a level close to that of the control group. The hyperphosphorylation of TAU protein is a common pathological characteristic of AD. As shown in Figure 3C and D, there is no significant difference in the expression level of TAU in the brain of mice in each group. Compared with the control group, the level of TAU phosphorylation in the brain of the AD model group was significantly increased. However, *L. casei* ATCC 393 or *L. casei* ATCC 393-SeNPs treatment significantly inhibited the TAU phosphorylation in the AD model mice, but *L. casei* ATCC 393-SeNPs was more effective than *L. casei* ATCC 393. Compared with the control group, the expression levels of caspase1 and Bax/Bcl in the brain of the AD model group were significantly increased, while the expression level of p53 was significantly decreased. Compared with the AD model group, dietary supplementation with *L. casei* ATCC 393 or *L. casei* ATCC 393-SeNPs decreased the expression level of caspase1 and Bax/Bcl-2, but the down-regulation effect of *L. casei* ATCC 393-SeNPs was more significant than *L. casei* ATCC 393. Moreover, *L. casei* ATCC 393-SeNPs significantly up-regulated the expression level of p53 in AD model mice (Figure 3E and F). These results indicated that *L. casei* ATCC 393-SeNPs administration suppressed A $\beta$  aggregation, hyperphosphorylation of TAU protein and neuronal apoptosis in AD model mice.

### *L. casei* ATCC 393-SeNPs Activated the Akt/CREB Signaling Pathway and Increased BDNF Expression

To explore the mechanisms underlying *L. casei* ATCC 393-SeNPs intervention ameliorating AD-like pathogenesis in AD model mice, we examined the expression of BDNF and the upstream signaling molecules Akt/CREB. As shown in Figure 4A and B, compared to the control group, the levels of the phosphorylation of Akt and CREB were significantly decreased, and the BDNF expression was down-regulated in AD model mice. While dietary supplementation with *L. casei* ATCC 393 or *L. casei* ATCC 393-SeNPs alleviated, the inhibitory effect of D-gal/AlCl<sub>3</sub> on protein phosphorylation of Akt and CREB, and on BDNF expression. The results indicated that the preventive effects of dietary supplementation with *L. casei* ATCC 393 or *L. casei* ATCC 393-SeNPs on D-gal/AlCl<sub>3</sub> induced AD-like pathogenesis was closely associated with its regulation on Akt/CREB/BDNF signaling pathway.

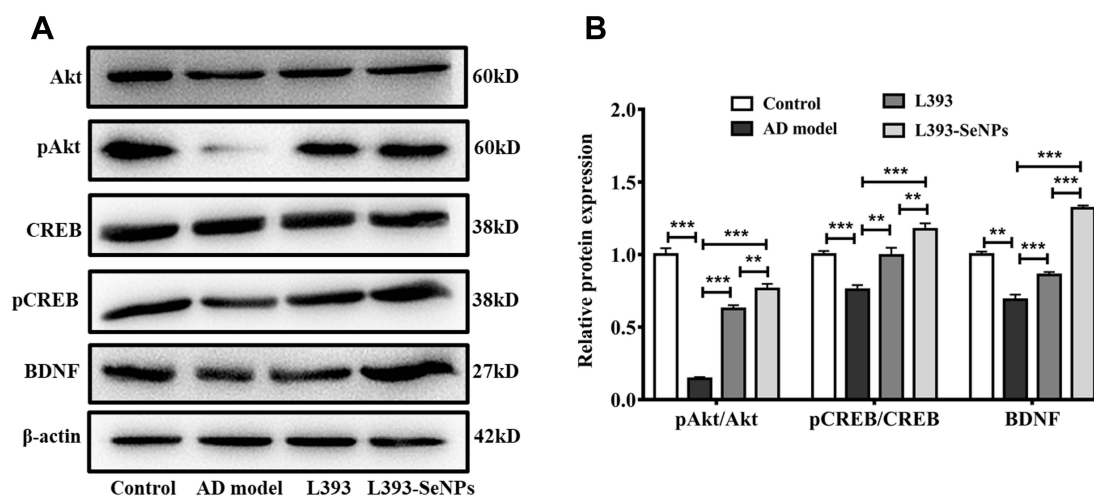


**Figure 4** *L. casei* ATCC 393-SeNPs activated the Akt/CREB signaling pathway and increased BDNF expression. (A) The expression levels of Akt, pAkt, CREB, pCREB and BDNF detected by Western blot analysis. (B) Quantitative analysis of the protein expression levels of pAkt/Akt, pCREB/CREB and BDNF. Data are represented as the mean  $\pm$  S.E.M. n=4. \*\*P < 0.01; \*\*\*P < 0.001 (L393: *L. casei* ATCC 393; L393-SeNPs: *L. casei* ATCC 393-SeNPs).

## Dietary Supplementation with *L. casei* ATCC 393-SeNPs Effectively Alleviated Intestinal Barrier Dysfunction in AD Model Mice

The intestinal barrier dysfunction is implicated in the occurrence and development of cognitive impairment in AD. We performed histological staining in the ileum. The images of H&E staining showed that compared with control group, AD model mice showed disordered ileal villi, shortened villus height, loss of crypts, and decreased the ratios of villus height to crypt depth, indicating that AD model mice had obviously impaired intestinal barrier integrity. *L. casei* ATCC 393 or *L. casei* ATCC 393-SeNPs treatment mitigated the magnitude of histological injuries in the ileum (Figure 5A–C). The detection of biomarkers related to intestinal barrier dysfunction, including FITC-dextran flux across intestinal epithelial cells and tight junction (TJ) proteins (ZO-1, occludin and claudin1) expression levels revealed that the level of serum FITC-dextran increased significantly and the levels of expression of TJ protein decreased significantly in AD model mice

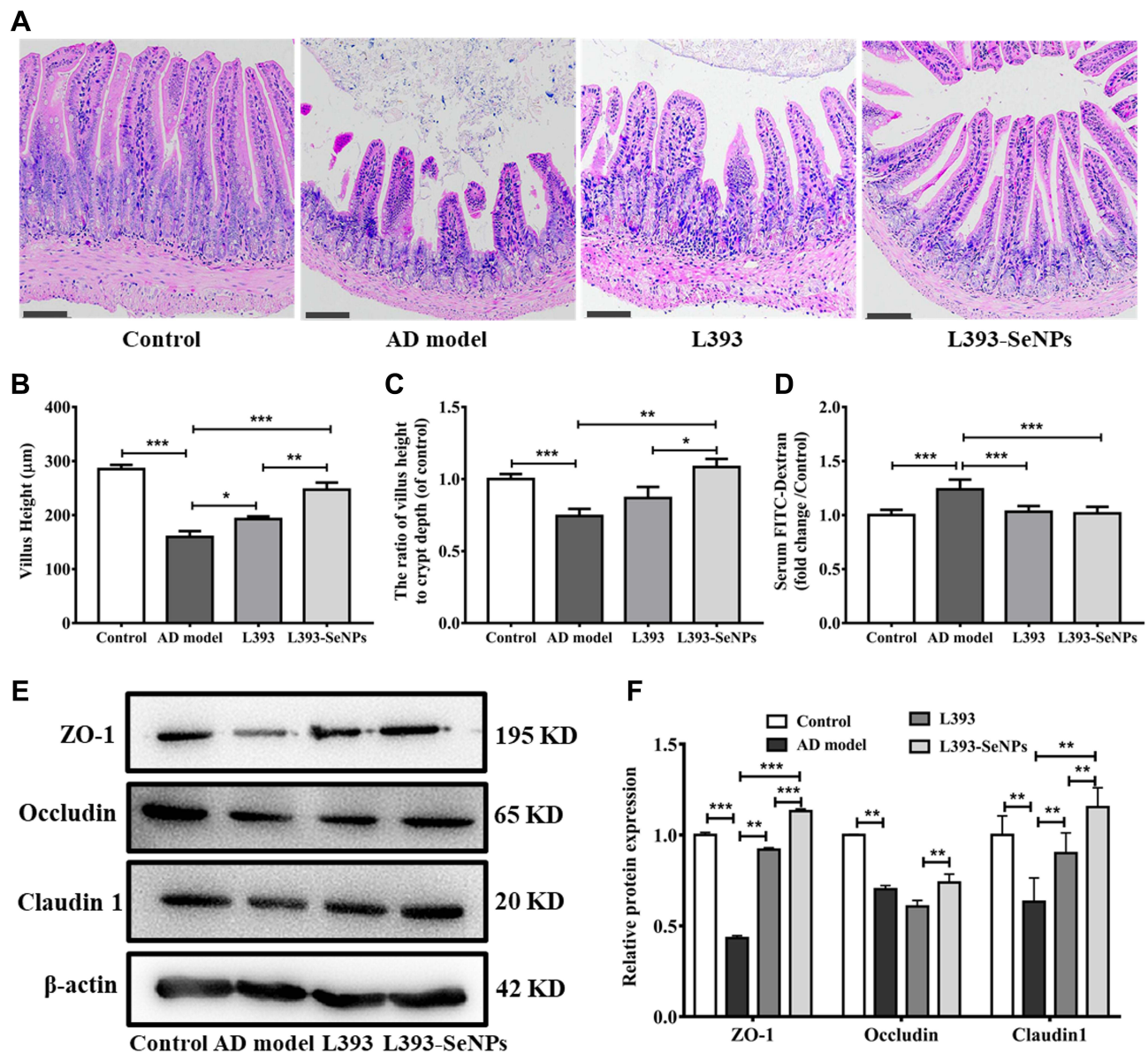


**Figure 5** Effects of *L. casei* ATCC 393-SeNPs on the intestinal barrier in AD model mice. (A) Ileal morphology was observed by H&E staining (Scale bar: 100 µm). (B) Villus height. (C) The ratio of villus height to crypt depth. (D) Serum FITC-Dextran content. (E) The expression levels of tight junction proteins (ZO-1, Occludin and Claudin 1) detected by Western blot analysis. (F) Quantitative analysis of the protein expression levels of ZO-1, Occludin and Claudin 1. Data are represented as the mean  $\pm$  S.E.M. n=6. \* $P < 0.05$ ; \*\* $P < 0.01$ ; \*\*\* $P < 0.001$  (L393: *L. casei* ATCC 393; L393-SeNPs: *L. casei* ATCC 393-SeNPs).

compared with the control group. Conversely, significantly increased levels of expression of TJ proteins and decreased level of FITC-dextran were observed in mice fed diet with *L. casei* ATCC 393 or *L. casei* ATCC 393-SeNPs compared with those in AD model group (Figure 5D–F).

## Effects of *L. casei* ATCC 393-SeNPs on the Inflammatory Response in AD Model Mice

The intestinal barrier dysfunction can trigger the inflammatory responses. To evaluate the effect of *L. casei* ATCC 393-SeNPs on neuroinflammation, brain samples were stained with the microglial marker IBA1. As shown in Figure 6A and B, IBA1 positive cells were significantly increased in brain of the AD model mice. *L. casei* ATCC 393 slightly suppressed activation of microglia. *L. casei* ATCC 393-SeNPs significantly reduced IBA1 immunoreactivity, exhibiting the strongest inhibitory effect on IBA1 expression. The activation of microglia will produce a lot of inflammation cytokines. The levels of IL-1 $\beta$  and IL-18 in the serum, brain and ileum of AD model mice were significantly higher than those in the control

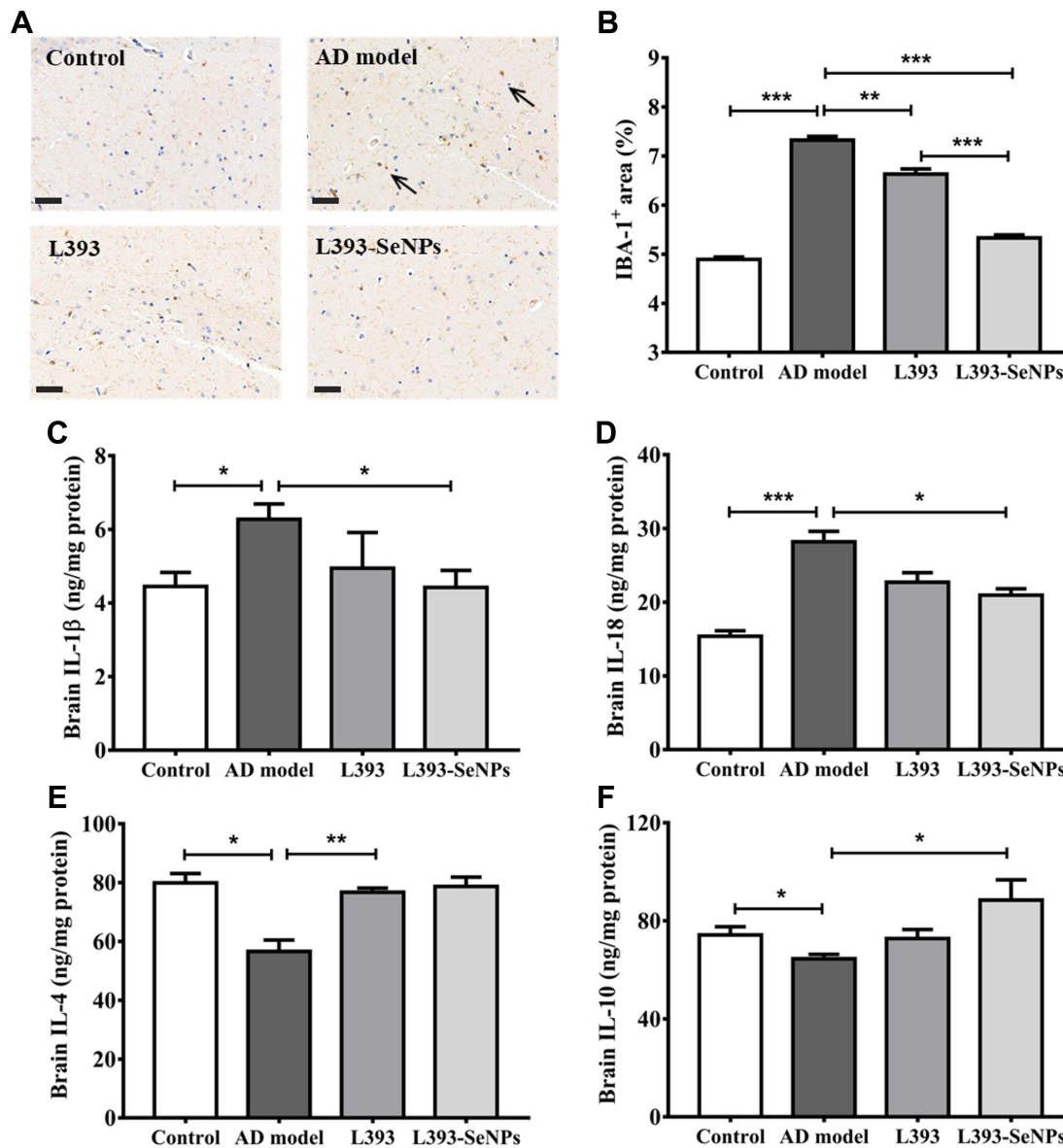


**Figure 6** Effects of *L. casei* ATCC 393-SeNPs on the immune response in the serum, brain and ileum of AD model mice. (A) The activated microglia in the brain of mice were detected by IBA-1 immunohistochem (Scale bar 50  $\mu$ m). (B) Quantitatively analysis by Image J software. (C) IL-1 $\beta$  level in brain. (D) IL-18 level in brain. (E) IL-4 level in brain. (F) IL-10 level in brain. Data are represented as the mean  $\pm$  S.E.M. n=6. \* $P$  < 0.05; \*\* $P$  < 0.01; \*\*\* $P$  < 0.001 (L393: *L. casei* ATCC 393; L393-SeNPs: *L. casei* ATCC 393-SeNPs).

group, and the levels of IL-4 and IL-10 in the brain were lower than that of the control group. Compared with *L. casei* ATCC 393 group, *L. casei* ATCC 393-SeNPs significantly reduced the levels of pro-inflammatory cytokines, and increased the levels of anti-inflammatory cytokines (Figure 6C–F, Figure S2A–D). These results suggested that *L. casei* ATCC 393-SeNPs inhibited overactivation of microglia and reduced the inflammatory response.

## Effects of *L. casei* ATCC 393-SeNPs on Se Content and the Antioxidant Capacity of AD Model Mice

The neuroprotective effect of *L. casei* ATCC 393-SeNPs may be related to the biological activity of Se. Thus, we detected the Se content in the organs, serum and feces by ICP-MS. Se concentration in liver, kidney, serum, ileum and feces of the *L. casei* ATCC 393-SeNPs was significantly higher than that in the AD model and *L. casei* ATCC 393 groups, and the Se content in brain of the *L. casei* ATCC 393-SeNPs group was higher than that in the AD model group (Figure S3A–F). Compared with the control group, the activities of T-SOD, GPx and TrxR were significantly decreased, while the level of MDA was significantly increased in the serum, brain and ileum of AD model group. Furthermore, *L. casei* ATCC 393-SeNPs exhibits stronger antioxidant capacity than *L. casei* ATCC 393, manifested in significantly increasing the activities of T-SOD, GPx and TrxR, and reducing the level of MDA in AD model mice (Figure 7A–D).

## *L. casei* ATCC 393-SeNPs Restored Gut Microbiota Balances in AD Model Mice

Gut microbiota plays a pivotal role in the onset and development of AD. As shown in Figure 8A and B, Chao1 and Observed species indices were significantly decreased in the AD model mice compared with the control group. AD model mice treated with *L. casei* ATCC 393-SeNPs significantly increased the Chao1 and Observed species indices. Compared with the control group, exogenous administration of D-gal and AlCl<sub>3</sub> significantly decreased Shannon index. AD model mice treated with *L. casei* ATCC 393-SeNPs has no effect on Shannon index of AD mice (Figure 8C). However, compared with *L. casei* ATCC 393 group, AD model mice treated with *L. casei* ATCC 393-SeNPs significantly increased the Chao1, observed species and Shannon indices. Those results indicated that dietary supplementation with *L. casei* ATCC 393-SeNPs effectively enhanced the diversity and abundance of microbial communities in AD model mice. The characteristic phylum-level microbiome was further compared among all groups based on the heatmaps (Figure 8D). Administration of D-gal and AlCl<sub>3</sub> led to an increase in the abundance of *Firmicutes* and decrease in the abundance of *Proteobacteria*, *TM7* and *Deferribacteres*. In addition, *L. casei* ATCC 393-SeNPs intervention increased the abundance of *Firmicutes* and *Actinobacteria*, and decreased the abundance of *Chloroflexi*, *Verrucomicrobia* and *Proteobacteria* in AD model mice. The Firmicutes/Bacteroidetes (F/B) ratio has been suggested as an important index of the health of the gut microbiota.<sup>31</sup> An increasing trend of the F/B ratio was observed in the AD model group compared with the control group. Conversely, *L. casei* ATCC 393-SeNPs treatment significantly reduced the F/B ratio compared with AD model and *L. casei* ATCC 393 groups, and reversed the gut microbiota imbalance (Figure 8E). At the genus level, compared with the control group, exogenous administration of D-gal and AlCl<sub>3</sub> led to significant increase in the abundance of *Aquabacterium*, *Parabacteroides*, *Sphingobium* and *Odoribacter*, and decrease in the abundance of *Adlercreutzia*, *Oscillospira*, *Mucispirillum* and *Streptococcus*. In addition, *L. casei* ATCC 393-SeNPs intervention decreased the abundance of *Parabacteroides*, *Sphingobium*, *Lactobacillus*, *Halomonas* and *Odoribacter*, and increased the abundance of *Allobaculum*, *Bifidobacterium*, *Turicibacter* and *Adlercreutzia* and when compared with the AD model group (Figure 8F and G). As shown in Figure 8H, the AD model group had low level of total SCFAs, acetate, isovalerate, and valerate when compared with the control group. However, *L. casei* ATCC 393-SeNPs intervention increased the total SCFAs, acetate, isovalerate, and valerate in AD model mice. Altogether, these data indicated that *L. casei* ATCC 393-SeNPs modified the microbiota composition and metabolism in AD model mice.

A heatmap of Spearman correlation between the altered genera in cecal contents and AD-related biochemical indexes (A $\beta$ <sub>1-42</sub>, AchE and the levels of neurotransmitters, inflammatory cytokines and antioxidant capacity in brain) was generated to identify the potential correlation between gut microbiota and AD. As shown in Figure 9, four bacteria genera (*Desulfovibrio*, *Halomonas*, *Sphingobium* and *Nitrosomonas*) were negatively correlated with the activity of GPx and *Allobaculum* was positively correlated with the activity of GPx. Moreover, *Sphingobium* positively correlated with

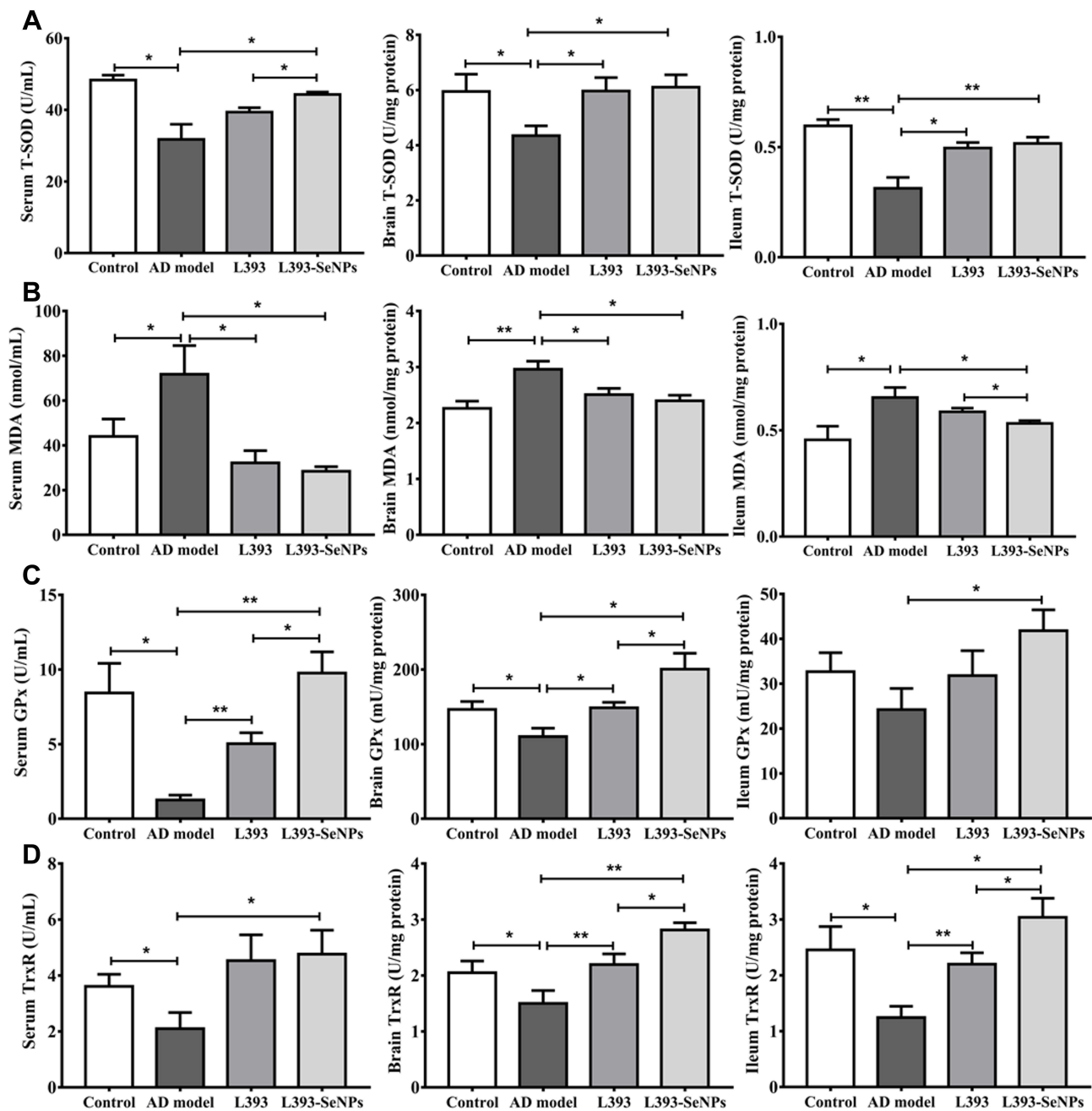


**Figure 7** Effects of *L. casei* ATCC 393-SeNPs on the antioxidant capacity of AD model mice. (A–D) Oxidative stress response including T-SOD (A), MDA (B), GPx (C) and TrxR (D). Data are represented as the mean ± S.E.M. n=6. \* $P < 0.05$ ; \*\* $P < 0.01$  (L393: *L. casei* ATCC 393; L393-SeNPs: *L. casei* ATCC 393-SeNPs).

pro-inflammatory cytokines and negatively correlated with anti-inflammatory cytokines. In addition, *Adlercreutzia*, *Streptococcus* and *Mucispirillum* were negatively correlated with  $A\beta_{1-42}$ , AchE, neurotransmitters and pro-inflammatory cytokines. It is worth noting that the abundance of *Adlercreutzia* significantly increased in the *L. casei* ATCC 393-SeNPs group, illustrating that *L. casei* ATCC 393-SeNPs effectively alleviated cognitive dysfunction in D-gal/ $AlCl_3$ -induced AD model mice. These results indicating that *L. casei* ATCC 393-SeNPs supplementation can alleviate oxidative stress and neuroinflammation by restoring gut microbiota balances.

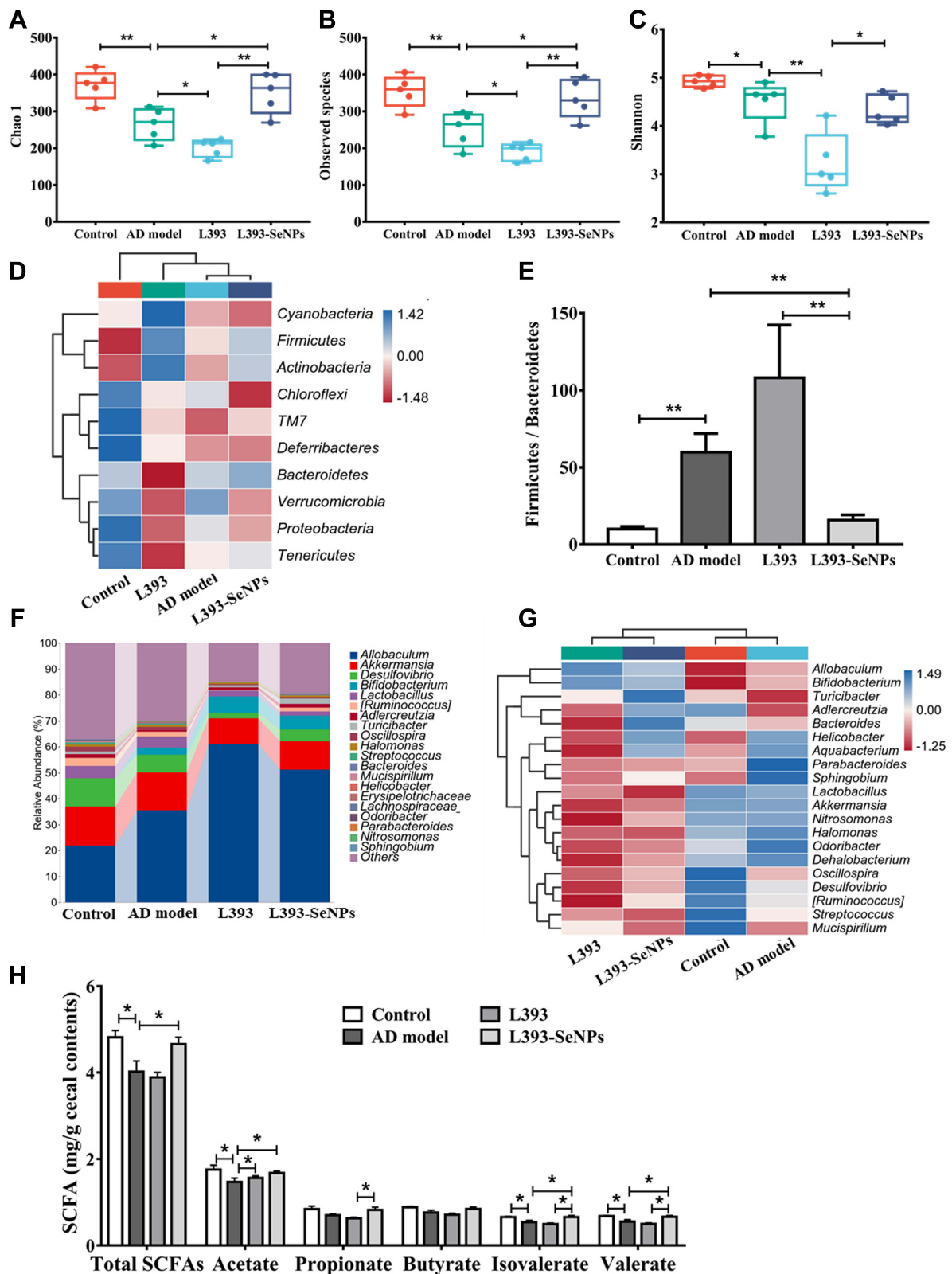


**Figure 8** Effects of *L. casei* ATCC 393-SeNPs on gut microbiota and SCFAs levels of AD model mice. (A–C) Alpha diversity index including Chao1 (A), Observed species (B) and Shannon (C). (D) Heatmap analysis at the phylum level. (E) Ratio of Firmicutes to Bacteroidetes. (F) The relative abundance composition of gut microbiota at the genus level. (G) Heatmap analysis at the genus level. (H) SCFAs levels in the cecal contents of mice. n=5. Data are represented as the mean ± S.E.M. \*P < 0.05; \*\*P < 0.01 (L393: *L. casei* ATCC 393; L393-SeNPs: *L. casei* ATCC 393-SeNPs).

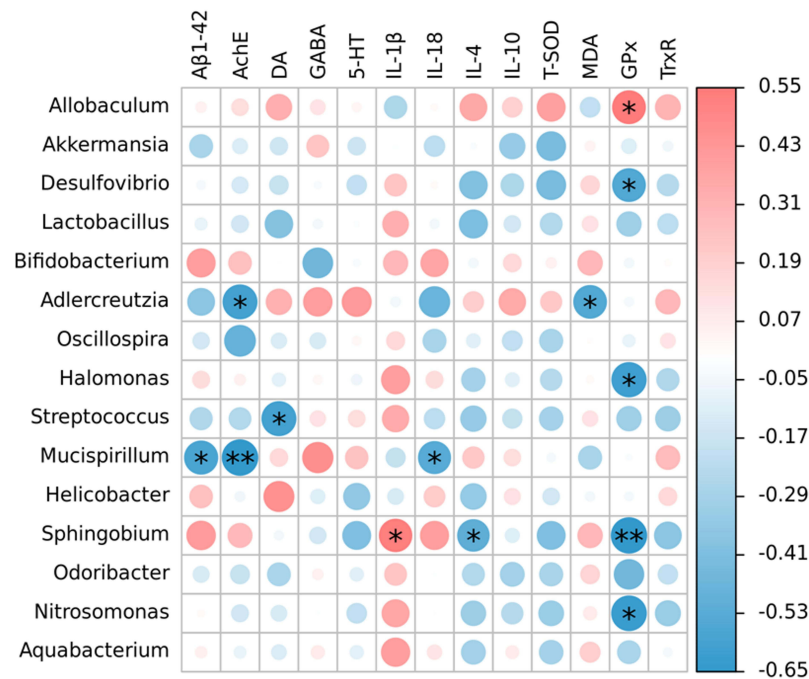


**Figure 9** Heatmap of Spearman correlation between the abundance of bacteria and the AD-related biochemical indexes. \* $P < 0.05$ ; \*\* $P < 0.01$ .

## Discussion

AD is a central neurodegenerative disease whose mechanism has not yet been clarified. Therefore, it is particularly important to establish an animal model that can reflect the pathogenesis of AD caused by natural aging in humans. Excessive D-gal can be metabolized into hydrogen peroxide and non-degradable galactitol, resulting in swelling of cells, increased osmotic pressure, destruction of cell membrane lipids, and metabolic disorders, triggering inflammatory responses and oxidative stress in the body, and ultimately leading to deterioration of multiple system functions, thereby rapidly inducing symptoms associated with natural aging.<sup>33,34</sup> Aluminum has significant neurotoxicity, can be combined with superoxide anion to form aluminum peroxide, and induce mitochondrial ROS production, which leads to accumulation of Aβ and oxidative stress in neuronal cells, and induces memory deficits related to AD pathogenesis.<sup>35</sup> Therefore, D-gal/AlCl<sub>3</sub>-induced Aβ plaque accumulation and cognitive impairment have been widely used as a model to study AD pathogenesis.<sup>33</sup> In this study, mice co-administered with D-gal and AlCl<sub>3</sub> exhibited significant memory deficits, manifested by prolonged escape latency, and increased swimming distance in MWM test. In addition, exogenous administration of D-gal and AlCl<sub>3</sub> significantly increased Aβ content and the level of TAU hyperphosphorylation in mice brain, which are the most representative pathological hallmarks of AD patients.<sup>3</sup>

Emerging evidence implicates that the gut microbiota can contribute to the pathogenesis of AD and influence normal physiological homeostasis through the microbiota-gut-brain axis.<sup>36</sup> The gut microbiota and specific bacteria can modulate neurotransmitter signaling in the central and peripheral systems by modulating neurotransmitters and their receptors.<sup>37</sup> For example, GABA is produced by most *Lactobacillus* and *Bifidobacterium* strains and GABA-producing probiotic strains influence health and behavior in animal models.<sup>38</sup> A recent study showed that *Lactobacillus paracasei* K71 intake could increase the levels of 5-HT in serum and brain tissue.<sup>39</sup> Similarly, our results found that dietary supplementation of *L. casei* ATCC 393 and *L. casei* ATCC 393-SeNPs could increase the levels of neurotransmitters in AD model mice to varying degrees, which may be related to gut microbiota. In the present study, a decrease in α-diversity and an increase in F/B ratio (an important index of the health of the gut microbiota) were observed in the AD model mice. Accumulating evidence suggested that AD histological and behavioral manifestations are correlated with gut microbiota dysbiosis.<sup>7</sup> In addition, evidence shows that gut barrier dysfunction may lead to impairment of bidirectional communication between the brain and gut. For instance, the

bacterial colonies of gut microbiota naturally release significant quantities of lipopolysaccharides, amyloids, and other inflammatory-related molecules, which leak from the intestinal tract and begin to accumulating at the systemic and brain levels, potentially causing neuroinflammation and contributing to AD.<sup>16</sup> Indeed, in our research, intestinal barrier dysfunction, microglial hyperactivation and elevated levels of inflammatory factors were observed in AD model mice.

Growing evidence suggests that probiotics have potential therapeutic in central nervous system (CNS)-related diseases, especially AD, due to their modulation of the microbiota-gut-brain axis. Preclinical and clinical studies have shown that *Bifidobacterium breve* A1 can prevent cognitive impairment in A $\beta$ -induced AD model rats and elderly people with mild cognitive impairment.<sup>40,41</sup> Yang et al demonstrated that combination of multiple probiotics substantially attenuated aging-related disruption of the intestinal barrier and blood-brain barrier, reduced plasma and cerebral lipopolysaccharides concentration, toll-like receptor 4 (TLR4) expression, and nuclear factor- $\kappa$ B (NF- $\kappa$ B) nuclear translocation in the brain.<sup>7</sup> In the 3xTg AD mouse model, administration of a combination of probiotics significantly improved sirtuin 1 (SIRT-1) neuroprotective protein levels and antioxidant status and diminished the protein carbonyl markers and oxidative stress markers in mouse brain.<sup>42</sup> Similarly, we also found that administration of *L. casei* ATCC 393 can improve cognitive impairment in AD mice to a certain extent, and reduce A $\beta$  brain aggregation and TAU hyperphosphorylation. In addition, many drugs have failed in clinical trials due to limited bioavailability, poor cellular and blood-brain barrier (BBB) permeability, and short drug half-lives. Nanoparticles-mediated drug delivery systems enhance drug solubility, bioavailability, and ability to cross the BBB, thus making them superior alternatives.<sup>43</sup> Currently, a variety of nanoparticles have been used in AD research. Gold nanoparticles inhibited A $\beta$  fibrillation, leading to the formation of fragmented fibrils and spherical oligomers and relieved A $\beta$ -mediated toxicity to neuroblastoma.<sup>44</sup> Siddiqui et al encapsulated resveratrol in glutathione-coated collagen nanoparticles' core and found that it had a favorable impact in reducing cognitive impairment in kindled mice.<sup>45</sup> In this study, we found that *L. casei* ATCC 393-SeNPs had better effects than *L. casei* ATCC 393 in improving cognitive impairment in AD model mice.

Se, as an essential nutrient trace element for biosynthesis of selenoprotein, plays a vital role in antioxidant and immune regulation.<sup>46</sup> Studies have pointed out that when the body develops inflammatory diseases, there will be a phenomenon of reduced selenium concentration and impaired selenoprotein synthesis, and the same phenomenon has also been found in AD patients.<sup>24,47</sup> Clinical trial results show that high-dose sodium selenate supplementation can increase the absorption of selenium in the central nervous system and improve the MMSE score, which is mainly due to the fact that Se can synthesize antioxidant selenoproteins, such as GPx and TrxR.<sup>27,48</sup> Shukla et al reported that in AD patients, GSH and GPx expression in both the frontal cortex and hippocampus is significantly down-regulated and correlated with the severity of injury.<sup>49</sup> Tamtaji et al found that multiple probiotics and Se combination improved MMSE score and some metabolic profiles in AD patients.<sup>25</sup> SeNPs have received extensive attention due to their unique biological properties and have been suggested as a safer and more effective platform for the delivery of Se for biological needs.<sup>28</sup> Our previous study demonstrated that *L. casei* ATCC 393 alleviated intestinal barrier dysfunction caused by *Enterotoxigenic Escherichia coli* K88 via TLRs-mediated mast cell pathway.<sup>50,51</sup> In addition, SeNPs synthesized by *L. casei* ATCC 393 possess significant antioxidant and anti-inflammatory activities in vitro and in vivo and dietary supplementation with SeNPs can prevent oxidative stress-induced intestinal barrier dysfunction through its regulation gut microbiota.<sup>29-31</sup> Thus, we evaluated the protective effects of *L. casei* ATCC 393-SeNPs against D-gal/AICl<sub>3</sub>-induced AD model mice. After *L. casei* ATCC 393-SeNPs intervention for 13 weeks, high concentration of Se was concentrated in liver, kidney, serum, brain, ileum and feces. Moreover, dietary supplementation with *L. casei* ATCC 393-SeNPs significantly increased the levels of neurotransmitters including DA, GABA, 5-HT, improved cognitive disorder, and inhibited A $\beta$  aggregation, TAU protein hyperphosphorylation, and neuronal apoptosis by enhancing the antioxidant capacity, and reducing the inflammatory response in AD model mice.

The protective effect of Se may be attributed to the ability of Se to modulate the gut microbiota to regulate intestinal barrier function and immune response.<sup>52</sup> We previously found Se deficiency resulted in a gut microbiota phenotype that was more susceptible to oxidative stress-induced intestinal barrier dysfunction and supernutritional SeNPs supplementation resulted in a gut microbiota phenotype that prevents the oxidative stress-induced intestinal barrier dysfunction.<sup>31</sup> In this study, *L. casei* ATCC 393-SeNPs significantly reduced the F/B ratio in AD model mice, and reversed the gut

microbiota imbalance. As a metabolite of the gut microbiota, similar alterations in the levels of SCFAs were also observed in the cecal contents of AD model. *L. casei* ATCC 393-SeNPs increased the content of total SCFAs, acetate, isovalerate, and valerate in AD model mice. Studies have shown that gut microbiota can synchronize the gut with the central nervous system by regulating the level of neurotransmitters and the synthesis of SCFAs, thereby regulating the immune homeostasis of the brain and participating in the pathogenesis of AD.<sup>16,53</sup> The concentrations of SCFAs are affected by the microbiota composition and abundance, dietary fiber content, and metabolic flux of SCFAs.<sup>36</sup> Recent studies have shown that SCFAs have protective effects on gut barrier function, preventing hippocampal neuroinflammation and neuronal damage induced by fructose diet.<sup>54</sup> Although the present study found that the protective effect of *L. casei* ATCC 393-SeNPs in AD model mice may be related to the regulation of gut microbiota, it could not prove that the effects are mediated predominantly by the gut microbiota, rather than direct effects in neurons. Thus, it should be demonstrated whether the beneficial effects of *L. casei* ATCC 393-SeNPs are abrogated in a gut microbiota-depleted AD model mice.

BDNF is widely expressed in the nervous system and its receptors, helps protect neurons, reduces necrosis and apoptosis of hippocampal neurons, and positively affects neuronal repair during neuronal chronic stress injury.<sup>55</sup> Increased A $\beta$  levels lead to a reduction of CREB phosphorylation and BDNF level, which contribute to the loss of synaptic plasticity and memory, as well as exacerbation of AD progression.<sup>56</sup> Preclinical studies have demonstrated that chronic administration of probiotics can reduce anxiety- and depressive-like behavior and can normalize associated physiological outputs, such as BDNF levels.<sup>57</sup> In this study, we found that the levels of the phosphorylation of Akt and CREB were significantly decreased and down-regulated BDNF expression in AD model mice. While dietary *L. casei* ATCC 393-SeNPs supplementation down-regulated the expression levels of p-Akt and p-CREB, and increased BDNF expression in AD model mice. BDNF has been reported to reduce neuronal apoptosis by upregulating the expression of Bcl-2 protein.<sup>58</sup>

Overall, biogenic SeNPs by *L. casei* ATCC 393 exhibit attractive properties in alleviating cognitive impairment. However, the nanosize of nanoparticles determines many of their beneficial properties and may also increase their potentially harmful effects. Therefore, it is necessary to assess the impact and interaction of nanoparticles with living systems before reaching their full potential.<sup>27</sup> Large rigid particles >2000 nm in diameter readily accumulate in the capillaries of the spleen, liver and lung; nanoparticles in the 100–200 nm diameter range leak through the fenestration of the tumor's blood vessels (enhanced permeability and retention effect) and escape the liver and spleen filtration; small-sized nanoparticles (<5 nm) are filtered out by the kidneys.<sup>59</sup> Therefore, the potential toxic effects caused by the continuous accumulation of nanoparticles deserve attention. Se has one of the smallest gaps between dietary deficiency and toxic levels, and toxicity of Se is mainly attributed to its inorganic form (selenite).<sup>60</sup> Even though the acute and chronic toxicity of SeNPs is far lower than that of sodium selenite, we should also pay attention to the poisoning phenomenon caused by the long-term accumulation of Se. Grotto et al found that long-term excessive Se supplementation induced hypertension in rats.<sup>61</sup> In addition, probiotics have many advantages and health benefits, but probiotic treatment also has risks, which are mainly related to the safety of vulnerable target groups.<sup>62</sup> A more critical challenge is to understand the mechanism of action of *L. casei* ATCC 393, to more specifically elucidate which health benefits *L. casei* ATCC 393 may provide, and to determine the intake required to achieve these effects. In conclusion, the toxicity and potential risks of *L. casei* ATCC 393-SeNPs must be fully evaluated before clinical trials are conducted.

## Conclusion

Overall, dietary supplementation with *L. casei* ATCC 393 or *L. casei* ATCC 393-SeNPs effectively alleviated cognitive dysfunction in D-gal/AICl<sub>3</sub>-induced AD model mice, and minimized A $\beta$  aggregation, hyperphosphorylation of TAU protein, and prevented neuronal death by Akt/CREB/BDNF signaling pathway. In addition, compared with *L. casei* ATCC 393, *L. casei* ATCC 393-SeNPs further effectively mitigated intestinal barrier dysfunction by improving antioxidant capacity, regulating immune response, restoring gut microbiota balance, and increasing the level of SCFAs and neurotransmitters, thereby inhibiting the activation of microglia and protecting brain neurons from neurotoxicity. Due to regulatory effects on microbiota-gut-brain axis, *L. casei* ATCC 393-SeNPs may be a promising and safe Se nutritional supplement for use as a food additive to prevent the AD-induced cognitive dysfunction.

## Abbreviations

5-HT, 5-hydroxytryptamine; AchE, acetylcholinesterase; AD, Alzheimer's disease; AlCl<sub>3</sub>, aluminum chloride; A $\beta$ , amyloid beta; BDNF, brain-derived neurotrophic factor; CREB, cAMP-response element binding protein; DA, dopamine; D-gal, D-galactose; GABA,  $\gamma$ -aminobutyric acid; GPx, glutathione peroxidase; IBA-1, ionized calcium-binding adapter molecule 1; ICP-MS, inductively coupled plasma-mass spectrometry; IL-10, interleukin-10; IL-18, interleukin-18; IL-1 $\beta$ , interleukin-1 $\beta$ ; IL-4, interleukin-4; *L. casei* ATCC 393, *Lactobacillus casei* ATCC 393; MCI, mild cognitive impairment; MDA, malondialdehyde; MMSE, mini-mental state examination; SCFAs, short-chain fatty acids; Se, Selenium; SeNPs, Se nanoparticles; SOD, superoxide dismutase; TrxR, thioredoxin reductase.

## Acknowledgments

This study was supported by the National Natural Science Foundation of China (No. 32072746) and the Innovation Foundation for Doctor Dissertation of Northwestern Polytechnical University (No. CX2021029 and No. CX2022062). The authors would like to thank Yafeng Zhang from Xi'an Institute for Food and Drug Control for ICP-MS measurement.

## Disclosure

The authors report no conflicts of interest in this work.

## References

1. Mufson EJ, Counts SE, Perez SE, Ginsberg SD. Cholinergic system during the progression of Alzheimer's disease: therapeutic implications. *Expert Rev Neurother*. 2008;8(11):1703–1718. doi:10.1586/14737175.8.11.1703
2. Shabbir U, Tyagi A, Elahi F, Aloo SO, Oh DH. The potential role of polyphenols in oxidative stress and inflammation induced by gut microbiota in alzheimer's disease. *Antioxidants*. 2021;10(9):1370. doi:10.3390/antiox10091370
3. Graham WV, Bonito-Oliva A, Sakmar TP. Update on alzheimer's disease therapy and prevention strategies. *Annu Rev Med*. 2017;68:413–430. doi:10.1146/annurev-med-042915-103753
4. Cheignon C, Tomas M, Bonnefont-Rousselot D, Faller P, Hureau C, Collin F. Oxidative stress and the amyloid beta peptide in Alzheimer's disease. *Redox Biol*. 2018;14:450–464. doi:10.1016/j.redox.2017.10.014
5. Selfridge JE, Lu EL. Role of mitochondrial homeostasis and dynamics in Alzheimer's disease. *Neurobiol Dis*. 2013;51:3–12. doi:10.1016/j.nbd.2011.12.057
6. Scheiblich H, Schlutter A, Golenbock DT, Latz E, Martinez-Martinez P, Heneka MT. Activation of the NLRP3 inflammasome in microglia: the role of ceramide. *J Neurochem*. 2017;143(5):534–550. doi:10.1111/jnc.14225
7. Yang X, Yu D, Xue L, Li H, Du J. Probiotics modulate the microbiota-gut-brain axis and improve memory deficits in aged SAMP8 mice. *Acta Pharm Sin B*. 2020;10(3):475–487. doi:10.1016/j.apsb.2019.07.001
8. Cenit MC, Sanz Y, Codoner-Franch P. Influence of gut microbiota on neuropsychiatric disorders. *World J Gastroenterol*. 2017;23(30):5486–5498. doi:10.3748/wjg.v23.i30.5486
9. Vogt NM, Kerby RL, Dill-McFarland KA, et al. Gut microbiome alterations in Alzheimer's disease. *Sci Rep*. 2017;7(1):13537. doi:10.1038/s41598-017-13601-y
10. Cattaneo A, Cattane N, Galluzzi S, et al. Association of brain amyloidosis with pro-inflammatory gut bacterial taxa and peripheral inflammation markers in cognitively impaired elderly. *Neurobiol Aging*. 2017;49:60–68. doi:10.1016/j.neurobiolaging.2016.08.019
11. Pellegrini C, Antonioli L, Colucci R, Blandizzi C, Fornai M. Interplay among gut microbiota, intestinal mucosal barrier and enteric neuro-immune system: a common path to neurodegenerative diseases? *Acta Neuropathol*. 2018;136(3):345–361. doi:10.1007/s00401-018-1856-5
12. Bostick JW, Mazmanian SK. Impaired gut barrier affects microglia health. *Nat Neurosci*. 2022;25(3):268–270. doi:10.1038/s41593-022-01028-2
13. Leitner GR, Wenzel TJ, Marshall N, Gates EJ, Klegeris A. Targeting toll-like receptor 4 to modulate neuroinflammation in central nervous system disorders. *Expert Opin Ther Targets*. 2019;23(10):865–882. doi:10.1080/14728222.2019.1676416
14. Hamanaka G, Kubo T, Ohtomo R, et al. Microglial responses after phagocytosis: Escherichia coli bioparticles, but not cell debris or amyloid beta, induce matrix metalloproteinase-9 secretion in cultured rat primary microglial cells. *Glia*. 2020;68(7):1435–1444. doi:10.1002/glia.23791
15. Huo JY, Jiang WY, Yin T, et al. Intestinal barrier dysfunction exacerbates neuroinflammation via the TLR4 pathway in mice with heart failure. *Front Physiol*. 2021;12:712338. doi:10.3389/fphys.2021.712338
16. Doifode T, Giridharan VV, Generoso JS, et al. The impact of the microbiota-gut-brain axis on Alzheimer's disease pathophysiology. *Pharmacol Res*. 2021;164:105314. doi:10.1016/j.phrs.2020.105314
17. Ji HF, Shen L. Probiotics as potential therapeutic options for Alzheimer's disease. *Appl Microbiol Biotechnol*. 2021;105(20):7721–7730. doi:10.1007/s00253-021-11607-1
18. Shaaban SY, El Gendy YG, Mehanna NS, et al. The role of probiotics in children with autism spectrum disorder: a prospective, open-label study. *Nutr Neurosci*. 2018;21(9):676–681. doi:10.1080/1028415X.2017.1347746
19. Akkasheh G, Kashani-Poor Z, Tajabadi-Ebrahimi M, et al. Clinical and metabolic response to probiotic administration in patients with major depressive disorder: a randomized, double-blind, placebo-controlled trial. *Nutrition*. 2016;32(3):315–320. doi:10.1016/j.nut.2015.09.003
20. Akbari E, Asemi Z, Daneshvar Kakhaki R, et al. Effect of probiotic supplementation on cognitive function and metabolic status in alzheimer's disease: a randomized, double-blind and controlled trial. *Front Aging Neurosci*. 2016;8:256. doi:10.3389/fnagi.2016.00256

21. Leblhuber F, Steiner K, Schuetz B, Fuchs D, Gostner JM. Probiotic supplementation in patients with alzheimer's dementia - an explorative intervention study. *Curr Alzheimer Res.* 2018;15(12):1106–1113. doi:10.2174/1389200219666180813144834
22. Deng H, Dong X, Chen M, Zou Z. Efficacy of probiotics on cognition, and biomarkers of inflammation and oxidative stress in adults with Alzheimer's disease or mild cognitive impairment - a meta-analysis of randomized controlled trials. *Aging-US.* 2020;12:4010–4039. doi:10.18632/aging.102810
23. Generoso JS, Giridharan VV, Lee J, Macedo D, Barichello T. The role of the microbiota-gut-brain axis in neuropsychiatric disorders. *Braz J Psychiatry.* 2021;43(3):293–305. doi:10.1590/1516-4446-2020-0987
24. Koc ER, Ilhan A, Zubeyde A, et al. A comparison of hair and serum trace elements in patients with Alzheimer disease and healthy participants. *Turk J Med Sci.* 2015;45(5):1034–1039. doi:10.3906/sag-1407-67
25. Tamtaji OR, Heidari-Soureshjani R, Mirhosseini N, et al. Probiotic and selenium co-supplementation, and the effects on clinical, metabolic and genetic status in Alzheimer's disease: a randomized, double-blind, controlled trial. *Clin Nutr.* 2019;38(6):2569–2575. doi:10.1016/j.clnu.2018.11.034
26. Cardoso BR, Roberts BR, Malpas CB, et al. Supranutritional sodium selenate supplementation delivers selenium to the central nervous system: results from a randomized controlled pilot trial in alzheimer's disease. *Neurotherapeutics.* 2019;16(1):192–202. doi:10.1007/s13311-018-0662-z
27. Qiao L, Dou X, Song X, Xu C. Green synthesis of nanoparticles by probiotics and their application. *Adv Appl Microbiol.* 2022;119:83–128.
28. Yang J, Yang H. Recent development in Se-enriched yeast, lactic acid bacteria and bifidobacteria. *Crit Rev Food Sci Nutr.* 2021;29:1–15.
29. Xu C, Qiao L, Guo Y, Ma L, Cheng Y. Preparation, characteristics and antioxidant activity of polysaccharides and proteins-capped selenium nanoparticles synthesized by *Lactobacillus casei* ATCC 393. *Carbohydr Polym.* 2018;195:576–585. doi:10.1016/j.carbpol.2018.04.110
30. Xu C, Guo Y, Qiao L, Ma L, Cheng Y, Roman A. Biogenic synthesis of novel functionalized selenium nanoparticles by *Lactobacillus casei* ATCC 393 and its protective effects on intestinal barrier dysfunction caused by enterotoxigenic *Escherichia coli* K88. *Front Microbiol.* 2018;9:1129. doi:10.3389/fmicb.2018.01129
31. Qiao L, Zhang X, Pi S, et al. Dietary supplementation with biogenic selenium nanoparticles alleviate oxidative stress-induced intestinal barrier dysfunction. *NPJ Sci Food.* 2022;6(1):30. doi:10.1038/s41538-022-00145-3
32. Halder N, Lal G. Cholinergic system and its therapeutic importance in inflammation and autoimmunity. *Front Immunol.* 2021;12:660342. doi:10.3389/fimmu.2021.660342
33. Liu CM, Ma JQ, Lou Y. Chronic administration of troxerutin protects mouse kidney against D-galactose-induced oxidative DNA damage. *Food Chem Toxicol.* 2010;48(10):2809–2817. doi:10.1016/j.fct.2010.07.011
34. Xu LQ, Xie YL, Gui SH, et al. Polydatin attenuates d-galactose-induced liver and brain damage through its anti-oxidative, anti-inflammatory and anti-apoptotic effects in mice. *Food Funct.* 2016;7(11):4545–4555. doi:10.1039/C6FO01057A
35. Huat TJ, Camats-Perna J, Newcombe EA, Valmas N, Kitazawa M, Medeiros R. Metal toxicity links to alzheimer's disease and neuroinflammation. *J Mol Biol.* 2019;431(9):1843–1868. doi:10.1016/j.jmb.2019.01.018
36. Zhong S-R, Kuang Q, Zhang F, Chen B, Zhong Z-G. Functional roles of the microbiota-gut-brain axis in Alzheimer's disease: implications of gut microbiota-targeted therapy. *Transl Neurosci.* 2021;12(1):581–600. doi:10.1515/tmsci-2020-0206
37. O'Mahony SM, Clarke G, Borre YE, Dinan TG, Cryan JF. Serotonin, tryptophan metabolism and the brain-gut-microbiome axis. *Behav Brain Res.* 2015;277:32–48. doi:10.1016/j.bbr.2014.07.027
38. Yunes RA, Poluektova EU, Dyachkova MS, et al. GABA production and structure of *gadB/gadC* genes in *Lactobacillus* and *Bifidobacterium* strains from human microbiota. *Anaerobe.* 2016;42:197–204. doi:10.1016/j.anaerobe.2016.10.011
39. Corpuz HM, Ichikawa S, Arimura M, et al. Long-term diet supplementation with *Lactobacillus paracasei* K71 prevents age-related cognitive decline in senescence-accelerated mouse prone 8. *Nutrients.* 2018;10(6):762. doi:10.3390/nu10060762
40. Kobayashi Y, Sugahara H, Shimada K, et al. Therapeutic potential of *Bifidobacterium breve* strain A1 for preventing cognitive impairment in Alzheimer's disease. *Sci Rep.* 2017;7(1):13510. doi:10.1038/s41598-017-13368-2
41. Kobayashi Y, Kinoshita T, Matsumoto A, Yoshino K, Saito I, Xiao JZ. *Bifidobacterium breve* A1 supplementation improved cognitive decline in older adults with mild cognitive impairment: an open-label, single-arm study. *J Prev Alzheimers Dis.* 2019;6(1):70–75. doi:10.14283/jpad.2018.32
42. Bonfili L, Cecarini V, Cuccioloni M, et al. SLAB51 probiotic formulation activates SIRT1 pathway promoting antioxidant and neuroprotective effects in an AD mouse model. *Mol Neurobiol.* 2018;55(10):7987–8000. doi:10.1007/s12035-018-0973-4
43. Hettiarachchi SD, Zhou Y, Seven E, et al. Nanoparticle-mediated approaches for Alzheimer's disease pathogenesis, diagnosis, and therapeutics. *J Control Release.* 2019;314:125–140. doi:10.1016/j.jconrel.2019.10.034
44. Liao YH, Chang YJ, Yoshiike Y, Chang YC, Chen YR. Negatively charged gold nanoparticles inhibit Alzheimer's amyloid-beta fibrillization, induce fibril dissociation, and mitigate neurotoxicity. *Small.* 2012;8(23):3631–3639. doi:10.1002/smll.201201068
45. Siddiqui MA, Akhter J, Bashir J, et al. Resveratrol loaded nanoparticles attenuate cognitive impairment and inflammatory markers in PTZ-induced kindled mice. *Int Immunopharmacol.* 2021;101:108287. doi:10.1016/j.intimp.2021.108287
46. Ala M, Kheyri Z. The rationale for selenium supplementation in inflammatory bowel disease: a mechanism-based point of view. *Nutrition.* 2021;85:111153. doi:10.1016/j.nut.2021.111153
47. Schomburg L. Selenium, selenoproteins and the thyroid gland: interactions in health and disease. *Nat Rev Endocrinol.* 2011;8(3):160–171. doi:10.1038/nrendo.2011.174
48. Carlisle AE, Lee N, Matthew-Onabanjo AN, et al. Selenium detoxification is required for cancer-cell survival. *Nat Metab.* 2020;2(7):603–611. doi:10.1038/s42255-020-0224-7
49. Shukla D, Mandal PK, Tripathi M, Vishwakarma G, Mishra R, Sandal K. Quantitation of in vivo brain glutathione conformers in cingulate cortex among age-matched control, MCI, and AD patients using MEGA-PRESS. *Hum Brain Mapp.* 2020;41(1):194–217. doi:10.1002/hbm.24799
50. Xu C, Yan S, Guo Y, et al. *Lactobacillus casei* ATCC 393 alleviates Enterotoxigenic *Escherichia coli* K88-induced intestinal barrier dysfunction via TLRs/mast cells pathway. *Life Sci.* 2020;244:117281. doi:10.1016/j.lfs.2020.117281
51. Song X, Pi S, Gao Y, et al. The role of vasoactive intestinal peptide and mast cells in the regulatory effect of *Lactobacillus casei* ATCC 393 on intestinal mucosal immune barrier. *Front Immunol.* 2021;12:723173. doi:10.3389/fimmu.2021.723173
52. Short SP, Pilat JM, Williams CS. Roles for selenium and selenoprotein P in the development, progression, and prevention of intestinal disease. *Free Radic Biol Med.* 2018;127:26–35. doi:10.1016/j.freeradbiomed.2018.05.066
53. Angelucci F, Cechova K, Amlerova J, Hort J. Antibiotics, gut microbiota, and Alzheimer's disease. *J Neuroinflammation.* 2019;16(1):108. doi:10.1186/s12974-019-1494-4

54. Li JM, Yu R, Zhang LP, et al. Dietary fructose-induced gut dysbiosis promotes mouse hippocampal neuroinflammation: a benefit of short-chain fatty acids. *Microbiome*. 2019;7(1):98. doi:10.1186/s40168-019-0713-7
55. Guo C, Liu Y, Fang MS, et al. omega-3PUFAs improve cognitive impairments through Ser133 phosphorylation of CREB upregulating BDNF/TrkB signal in schizophrenia. *Neurotherapeutics*. 2020;17(3):1271–1286. doi:10.1007/s13311-020-00859-w
56. Lei H, Zhang Y, Huang L, et al. L-3-n-butylphthalide regulates proliferation, migration, and differentiation of neural stem cell in vitro and promotes neurogenesis in APP/PS1 mouse model by regulating BDNF/TrkB/CREB/Akt pathway. *Neurotox Res*. 2018;34(3):477–488. doi:10.1007/s12640-018-9905-3
57. Bercik P, Denou E, Collins J, et al. The intestinal microbiota affect central levels of brain-derived neurotrophic factor and behavior in mice. *Gastroenterology*. 2011;141(2):599–609. doi:10.1053/j.gastro.2011.04.052
58. Li LX, Chu JH, Chen XW, et al. Selenium ameliorates mercuric chloride-induced brain damage through activating BDNF/TrkB/PI3K/AKT and inhibiting NF-kappaB signaling pathways. *J Inorg Biochem*. 2022;229:111716. doi:10.1016/j.jinorgbio.2022.111716
59. Blanco E, Shen H, Ferrari M. Principles of nanoparticle design for overcoming biological barriers to drug delivery. *Nat Biotechnol*. 2015;33(9):941–951. doi:10.1038/nbt.3330
60. Vinković Vrček I. Selenium nanoparticles: biomedical applications. In: Michalke B, editor. Selenium. Cham: Springer International Publishing; 2018:393–412.
61. Grotto D, Carneiro MFH, de Castro MM, Garcia SC, Barbosa Junior F. Long-term excessive selenium supplementation induces hypertension in rats. *Biol Trace Elem Res*. 2018;182(1):70–77. doi:10.1007/s12011-017-1076-1
62. Ayichew T, Belete A, Alebachew T, Tsehaye H, Berhanu H, Minwuyelet A. Bacterial probiotics their importances and limitations: a review. *J Nutr Health Sci*. 2017;4:2.

International Journal of Nanomedicine

Dovepress

## Publish your work in this journal

The International Journal of Nanomedicine is an international, peer-reviewed journal focusing on the application of nanotechnology in diagnostics, therapeutics, and drug delivery systems throughout the biomedical field. This journal is indexed on PubMed Central, MedLine, CAS, SciSearch®, Current Contents®/Clinical Medicine, Journal Citation Reports/Science Edition, EMBase, Scopus and the Elsevier Bibliographic databases. The manuscript management system is completely online and includes a very quick and fair peer-review system, which is all easy to use. Visit <http://www.dovepress.com/testimonials.php> to read real quotes from published authors.

Submit your manuscript here: <https://www.dovepress.com/international-journal-of-nanomedicine-journal>